

Article

Multi-Criterion Analysis of Cyclone Risk along the Coast of Tamil Nadu, India—A Geospatial Approach

Subbarayan Saravanan ¹, Devanantham Abijith ¹, Parthasarathy Kulithalai Shiyam Sundar ², Nagireddy Masthan Reddy ¹, Hussein Almohamad ^{3,*}, Ahmed Abdullah Al Dughairi ³, Motrih Al-Mutiry ⁴ and Hazem Ghassan Abdo ⁵

¹ Department of Civil Engineering, National Institute of Technology, Tiruchirappalli 620015, India; ssaravanan@nitt.edu (S.S.); abijith9007@gmail.com (D.A.); masthanreddy64@gmail.com (N.M.R.)

² Department of Water Resources and Ocean Engineering, National Institute of Technology, Mangaluru 575025, India; parthas1993@gmail.com

³ Department of Geography, College of Arabic Language and Social Studies, Qassim University, Buraydah 51452, Saudi Arabia; adgierie@qu.edu.sa

⁴ Department of Geography, College of Arts, Princess Nourah bint Abdulrahman University, Riyadh 11671, Saudi Arabia; mkalmutairy@pnu.edu.sa

⁵ Geography Department, Faculty of Arts and Humanities, Tartous University, Tartous P.O. Box 2147, Syria; hazemabdo@tartous-univ.edu.sy

* Correspondence: h.almohamad@qu.edu.sa

Abstract: A tropical cyclone is a significant natural phenomenon that results in substantial socio-economic and environmental damage. These catastrophes impact millions of people every year, with those who live close to coastal areas being particularly affected. With a few coastal cities with large population densities, Tamil Nadu's coast is the third-most cyclone-prone state in India. This study involves the generation of a cyclone risk map by utilizing four distinct components: hazards, exposure, vulnerability, and mitigation. The study employed a Geographical Information System (GIS) and an Analytical Hierarchical Process (AHP) technique to compute an integrated risk index considering 16 spatial variables. The study was validated by the devastating cyclone GAJA in 2018. The resulting risk assessment shows the cyclone risk is higher in zones 1 and 2 in the study area and emphasizes the variations in mitigation impact on cyclone risk in zones 4 and 5. The risk maps demonstrate that low-lying areas near the coast, comprising about 3%, are perceived as having the adaptive capacity for disaster mitigation and are at heightened risk from cyclones regarding population and assets. The present study can offer valuable guidance for enhancing natural hazard preparedness and mitigation measures in the coastal region of Tamil Nadu.

Keywords: cyclone vulnerability; risk assessment; GIS; remote sensing; AHP; Tamil Nadu



Citation: Saravanan, S.; Abijith, D.; Kulithalai Shiyam Sundar, P.; Reddy, N.M.; Almohamad, H.; Al Dughairi, A.A.; Al-Mutiry, M.; Abdo, H.G. Multi-Criterion Analysis of Cyclone Risk along the Coast of Tamil Nadu, India—A Geospatial Approach. *ISPRS Int. J. Geo-Inf.* **2023**, *12*, 341. <https://doi.org/10.3390/ijgi12080341>

Academic Editors: Diego González-Aguilera, Pablo Rodríguez-Gonzálvez and Wolfgang Kainz

Received: 3 June 2023

Revised: 9 August 2023

Accepted: 11 August 2023

Published: 16 August 2023



Copyright: © 2023 by the authors. Licensee MDPI, Basel, Switzerland. This article is an open access article distributed under the terms and conditions of the Creative Commons Attribution (CC BY) license (<https://creativecommons.org/licenses/by/4.0/>).

1. Introduction

Tropical cyclones are powerful natural disasters characterized by strong winds, heavy rainfall, storm surges, and flooding [1,2]. They form over warm ocean waters near the equator, where the sea surface temperature is at least 26.5 °C, and can reach wind speeds up to 200 miles per hour [3]. The storm rotates around a calm eye, ranging from a few miles to over 100 miles in diameter. Cyclones in the North Atlantic and Northwestern Pacific are classified on the Saffir-Simpson Hurricane Wind Scale, ranging from Category 1 to Category 5, which estimates the potential damage of the cyclone [4]. In India, Indian Meteorological Department (IMD) Cyclone Intensity Scale of eight classes are used namely Low Pressure (Less than 31 km/h), Depression (31–49 km/h), Deep Depression (50–61 km/h), Cyclonic Storm (62–88 km/h), Severe Cyclonic Storm (89–117 km/h), Very Severe Cyclonic Storm (118–167 km/h), Extremely Severe Cyclonic Storm (168–221 km/h) and Super Cyclonic Storm (More than 222 km/h) [5]. Annually, cyclones with strong wind velocity and storm

surge damage property, livelihoods, human lives, and the natural environment all around the globe [6]. Global climate change causes substantial increases in ocean temperatures, resulting in an increased frequency of more severe events worldwide [7]. Intense tropical cyclones possess destructive characteristics attributable to their mighty surface-level winds, extensive precipitation, and the resulting storm surge. Consequently, they have the capacity to inflict significant harm upon agriculture, properties, and livelihoods, resulting in substantial economic losses. Every year, 80–100 destructive tropical cyclones strike various parts of the world, affecting approximately 20,000 people and causing massive economic losses estimated at 6–7 billion USD [8,9].

Climate change scenarios make coastal populations and the environment more vulnerable to tropical cyclones. The portion of strong tropical cyclones is anticipated to rise further with greater wind speeds, higher storm surges, and extreme rainfall [10,11]. Most climate model studies predict a decline in the proportion of low-intensity cyclones. Hence, the annual total number of tropical cyclones is anticipated to fall or remain approximately constant [12]. Estimates predict that tropical cyclone intensities will rise in the twenty-first century if global warming and climate change continue on their current paths. Within 100 km of the storm eye, wind speeds are expected to rise by 10% and precipitation rates to rise by nearly 20%. The behavior of tropical cyclones is predicted to vary in two ways because of climate change. First, these storms usually form when the ocean surface is very warm and there is a strong temperature gradient between the surface and the upper atmosphere [13]. The gradient will likely weaken as the earth's temperature rises, making it less conducive for tropical cyclones to form. Second, higher ocean surface temperatures can increase cyclones' energy, resulting in stronger winds and more intense rainfall. As a result, the overall number of tropical cyclones is anticipated to decrease, but those that do form may be more powerful and destructive [14].

The Intergovernmental Panel on Climate Change (IPCC) has established a framework wherein vulnerability can be defined as a combination of exposure, sensitivity, and adaptive capacity. Exposure relates to households, assets, and properties in areas vulnerable to potential hazards, which may lead to adverse consequences such as damage or loss. The utilization of the sensitivity concept may describe the diverse levels of susceptibility exhibited by exposed components concerning loss and depletion. The term adaptive capacity applies to the ability of an individual, household, or community to build resilience and adapt to potential hazards [15]. The cyclone risk assessment was based on several key factors, including the intensity of the hazard, the level of population exposure, the degree of poverty, and the level of governance [16]. The impact of population exposure on mortality risk escalates with the intensity of the tropical cyclone [17]. Implementing suitable mitigation strategies can decrease severe tropical cyclones' negative consequences and effects. A thorough evaluation of vulnerability to tropical cyclones can yield adequate data to facilitate the implementation of efficient mitigation strategies [18,19].

The enhanced ability to forecast the trajectory and intensity of cyclones that have emerged over the Bay of Bengal and Arabian Sea in India over the past decade is indicative of the increasing expertise in this domain. Nevertheless, the implementation of more comprehensive preparedness measures would invariably enhance our ability to mitigate the detrimental effects of cyclones. Therefore, it is imperative to comprehensively understand the susceptibility of every region within the country by utilizing contemporary datasets and sophisticated technologies such as remote sensing and Geographic Information Systems (GIS). The Bay of Bengal is highly conducive to forming tropical cyclones, which occur five to six times more frequently than in the Arabian Sea. A comprehensive analysis of cyclones formed in the Bay of Bengal from 1881 to 1990, spanning over a century, indicates that around 14% made landfall in Bangladesh, while approximately 66% hit India. Notably, although the Bay of Bengal accounts for 10% of the world's cyclones, only 1.4% of the total cyclones affected Bangladesh, while the rest impacted India [20,21]. Cyclonic systems are a common occurrence in the North Indian Ocean, particularly during the pre-monsoon (March–May) and post-monsoon (October–December) seasons [22]. The number of tropical

cyclones in the post-monsoon season is higher, and the associated rainfall contributes to approximately 60% of the total annual precipitation in the various coastal states of Orissa, West Bengal, Tamil Nadu, and Andhra Pradesh [23] that are present along the Bay of Bengal. The extreme rainfall associated with tropical cyclones can result in significant hazards [24]. The excessive population concentration, which amounts to 40% of India's total population, lives within 100 km of the coastline, and tropical cyclones harm approximately 340 million people annually [25].

Geospatial techniques involving remote sensing and spatial analysis can be effective tools for modeling tropical cyclone hazards. This approach can be enhanced by integrating local knowledge and expertise, resulting in a simplified yet comprehensive methodology [26]. Previous research has been carried out related to cyclones, focusing on assessing the perception of cyclone risk, vulnerability, impacts, and adaptation. A substantial quantity of pertinent qualitative and quantitative information is imperative to generate a comprehensive database for an efficacious evaluation of cyclone risk [27]. To achieve optimal outcomes, integrating vulnerability and exposure assessments of both natural and anthropogenic factors is necessary. According to Mohapatra [22], several regions in India are at a higher risk of experiencing cyclone hazards, particularly those located on the east coast, including Tamil Nadu, Andhra Pradesh, Orissa, and West Bengal, as well as the Union Territory of Puducherry. Additionally, Gujarat, situated on the west coast, is susceptible to severe cyclones.

Multiple Criteria Decision Analysis (MCDA) is a decision support technique that facilitates the process of structuring, evaluating, and quantifying a decision problem [28]. Shankar et al. [29] aimed to identify flood-prone areas due to the Lehar cyclone in the southern part of South Andaman, India, and used four parameters—Land Use and Land Cover (LULC), geomorphology, slope, and demographic data—and multi-criteria weighted overlay analysis techniques for finding the cyclone vulnerability. Mansour et al. [30] employed a GIS and an Analytical Hierarchical Process (AHP) methodology to compute an integrated tropical cyclone risk. The index was based on a geodatabase comprising 17 variables and was conducted along the northeast coast of Oman. Hoque, M.A.A. et al. [19] analyzed the spatial distribution of vulnerability to tropical cyclones in the western coastal region of Bangladesh using the Fuzzy Analytical Hierarchy Process (FAHP) to generate indices for physical vulnerability, social vulnerability, and mitigation capacity of tropical cyclones. Even though tropical cyclones cause a disproportionately high number of occurrences, calamities, and damages to properties and environments, very few studies are linked to tropical cyclone risk mapping in India. Various studies [5,26,31–35] around the globe utilized the MCDA technique in the management of natural disasters and found it to be extensive. However, it has been observed that there has been a lack of literature reviews on the implementation of MCDA in the various phases of disaster management, including mitigation, preparedness, response, and recovery [36]. Malak et al. [37] examined the adaptive strategies employed by elderly individuals in response to cyclones in Bangladesh. Walsh [38] elucidates the institutional determination to disregard the vulnerability issue in the early warning system during the year 1892, and the study contributes to the existing literature that emphasizes the significance of recognizing the enduring nature of disasters in comprehending the emergence and persistence of vulnerability trajectories over time. Numerous academic articles on vulnerability have underscored the significance of integrating social and economic assets alongside physical and biophysical dimensions of vulnerability to natural hazards [33,34,39–42].

This research aims to develop a comprehensive tropical cyclone risk map that incorporates hazards, vulnerability, exposure, and mitigation using AHP and geospatial techniques. This study also attempts to examine the risk of cyclones without mitigation measures and their impact on coastal regions by exploring the spatial distribution of tropical cyclone vulnerability on the east coast of Tamil Nadu, India. The intended outcome is to quantify the level of risk associated with tropical cyclone impacts in the region. The findings of this study will provide valuable insights for policymakers across various governmental tiers in

their endeavors to develop a universally applicable strategy for mitigating the risks posed by natural hazards, ensuring inclusivity for individuals irrespective of their geographical location, racial background, or other distinguishing attributes.

2. Materials and Methods

2.1. Study Area

The Tamil Nadu coastline is situated on the southeastern region of the Indian Peninsula, comprising a segment of the Coromandel Coast that borders the Bay of Bengal in the east, the Indian Ocean in the south, and the Arabian Sea in the west. With a length of 1076 km, this coastline ranks second-longest in the country, after Gujarat. The study area has been classified into five zones (Figure 1) based on the magnitude and type of hazard, as well as the orientation of land towards the ocean. The zone 1 and 2 are severely affected by cyclones, resulting in heavy precipitation and coastal flooding. Due to the geographic location of the region, the zone 3 and 4 do not bear a heavy toll on these hazards. The zone 5 is impacted by storm surges and coastal flooding. The lands of these five zones have different orientations towards the coast, and the effect of littoral drift also varies with the transportation of sediments along the segments. Zones 1 to 4 fall in the Bay of Bengal, whereas zone 5 is shared by the Bay of Bengal, the Indian Ocean, and the Arabian Sea. Chennai, the state's capital, is a significant hub for commercial activities and industries within the nation. It is situated in the northern region of the coastal area, while Kanyakumari marks the southernmost point where the Indian Ocean, the Bay of Bengal, and the Arabian Sea converge. Along the Palk Strait in the Gulf of Mannar, it has a maritime boundary with Sri Lanka. The coastal corridor encompasses 14 districts and features 15 prominent ports, harbors, and various sandy beaches, lakes, and river estuaries. Tamil Nadu is the only state in India that possesses land on the southern, eastern, and western coastlines. The coastal region begins at Pazhaverkadu in the Thiruvallur district and ends at Ezhudesam in the Kanniyakumari district. Kanniyakumari is situated at the southernmost point of the Indian subcontinent, where the three waters meet. With an average temperature of 22.4 °C and a maximum temperature of 31.5 °C, it has a semi-arid tropical monsoon climate. After the monsoon period, the area experiences the highest precipitation from October to December. There are indications of a rise in intense rainfall during the northeast monsoon season and a minor decline during the southwest monsoon season [43]. The study area encompasses diverse natural habitats, such as sandy beaches, rocky coasts, and muddy flats, in addition to its distinctive geography and climate. Despite the limited distribution of natural habitats, Pichavaram, the world's second-largest mangrove forest, is situated on the coast of the Cuddalore district near Chidambaram [44,45]. The Bay of Bengal, located along the coastal region, is widely recognized as the site of the most powerful and fatal tropical cyclones globally. Tsunamis, such as the one that occurred in the Indian Ocean in 2004, resulting in the loss of over 10,000 lives and the displacement of hundreds of thousands of individuals, are great reminders of the devastating impact of these natural disasters [46–48].

2.2. Data Sources

A geodatabase has been developed to evaluate the coast's vulnerability to cyclones, including spatial layers and attribute datasets from various sources (Table 1). By utilizing GIS and spatial analysis tools, diverse spatial and demographic data layers were transformed into spatial data. The present study utilized the methodology depicted in Figure 2. The decision criteria for cyclone hazards, vulnerability, exposure, mitigation, and risk assessment have been carried out. The process of determining the weight of each factor selected was carried out through Saaty's Analytic Hierarchy Process (AHP) method. The utilization of weighted overlay analysis was employed to integrate the spatial database in order to analyze cyclone risk.

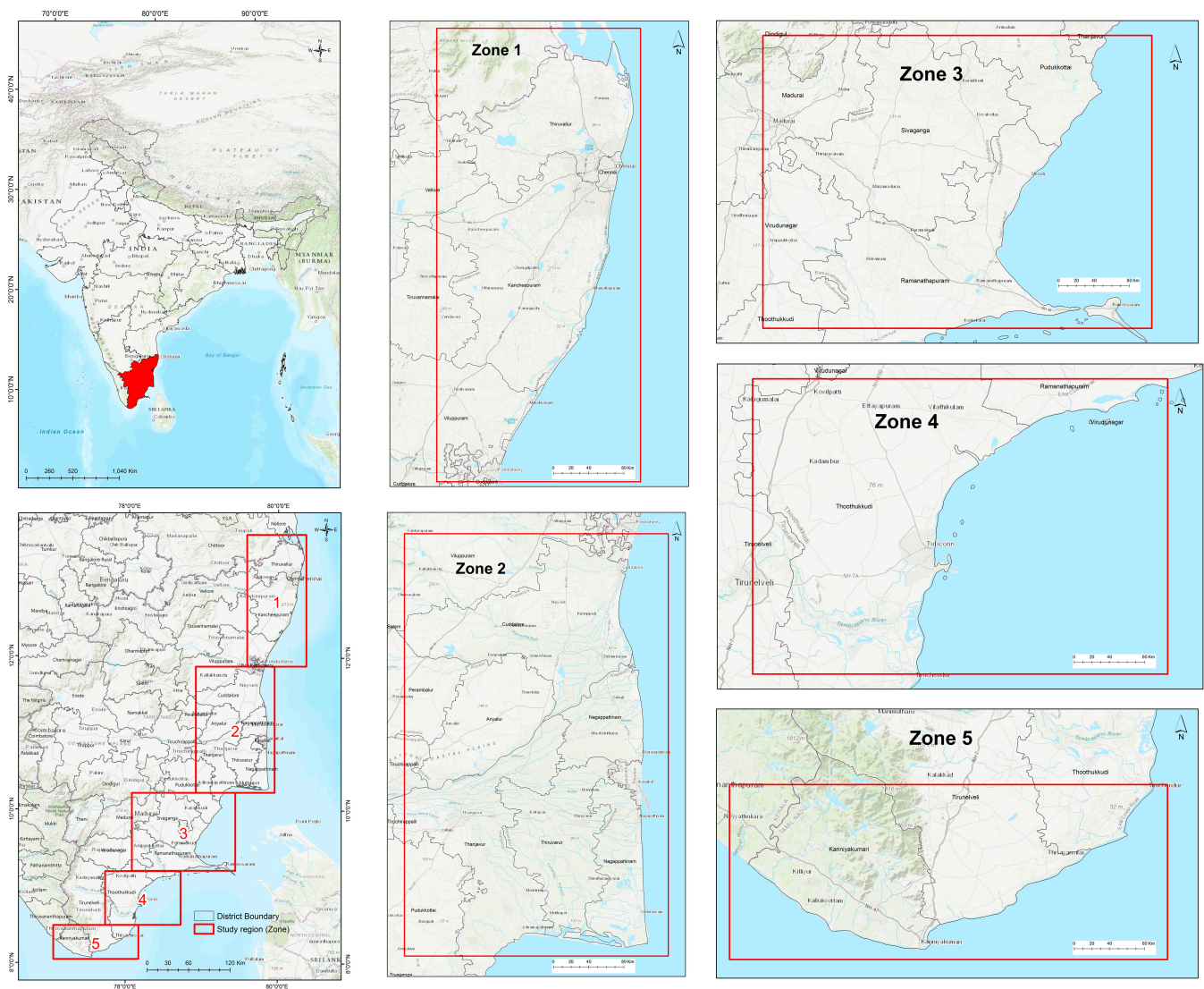


Figure 1. Shows the geographical region for study, which has been divided into five distinct zones.

2.3. Previous Cyclones in the Study Area

The National Cyclone Risk Mitigation Project (NCRMP) categorizes the cyclone-prone area into two categories based on the frequency of cyclone occurrence, population size, and the extent of institutional mechanisms for disaster management. Andhra Pradesh, Gujarat, Odisha, Tamil Nadu, and West Bengal have the highest vulnerability, falling under category I, whereas category II states include Maharashtra, Karnataka, Kerala, Goa, Pondicherry, Lakshadweep, Daman and Diu, and the Andaman and Nicobar Islands. Figure 3a depicts the previous major cyclones that crossed India. Figure 3b shows that the cyclonic storms crossed between 1980 and 2021 in the study area. From IMD cyclone reports, a few cyclones and their effects are discussed.

Many severe cyclones have occurred in the Bay of Bengal, resulting in a huge surge of up to 1–1.5 m in average along Chennai, Nagapattinam, Thanjavur, Cuddalore, Thondi, Rameshwaram, Ramanathapuram, Kilakkarai, and Rochemary Island between 1940 and 2005, resulting in severe damage to properties and human lives. Some of the recent cyclones, including Cyclonic Storm Baaz (November 2005), originated near the Andaman and Nicobar Islands. Baaz made two landfalls, one over the Andaman and Nicobar Islands and one over Tamil Nadu, just north of Puducherry. Both of its landfalls were below cyclone intensity. Cyclone Fanoos (December 2005) caused severe to localized devastating flooding across the area in and around areas of northern Sri Lanka and coastal Tamil Nadu state [49].

Moving westward, it attained peak intensity with 85 km/h winds and made landfall near Vedaranyam, Tamil Nadu. The storm was known for its excessive rainfall. Cyclonic Storm Nisha (November 2008) formed near northern Sri Lanka and moved inland near Karaikal with a maximum wind speed of 85 km/h. The storm brought heavy rainfall, which resulted in 189 deaths in Tamil Nadu. Severe Cyclonic Storm Jal (November 2010) hit Chennai as a deep depression with maximum winds of 110 km/h.

Table 1. Data sources of both primary and secondary data.

Parameters	Data Source	Source Location
Cyclone intensity	The International Best Track Archive for Climate Stewardship (IBTrACS) and IMD	https://www.ncei.noaa.gov/products/international-best-track-archive (accessed on 15 January 2023)
Cyclone frequency		http://www.rsmcnewdelhi.imd.gov.in/ (accessed on 20 January 2023)
Cyclone Path		
LULC	Landsat 8	Google Earth Engine (GEE) https://code.earthengine.google.com/ (accessed on 20 January 2023)
Elevation	Shuttle Radar Topography Mission (SRTM)	
Slope		
NDVI	Landsat 8	
Rainfall	IMD	https://www.imdpune.gov.in/ (accessed on 22 January 2023)
Road Network	OpenStreetMap (OSM)	https://www.openstreetmap.org (accessed on 29 January 2023)
Stream Network		
Distance to shoreline	Coastline	https://www.ngdc.noaa.gov (accessed on 31 January 2023)
Population Density	NASA's Socio-economic Data and Applications Center (SEDAC)	https://sedac.ciesin.columbia.edu/ (accessed on 6 February 2023)
Literacy rate		
Household density		
Distance from a cyclone shelter	Google Earth	https://earth.google.com/ (accessed on 10 February 2023)
Distance to the health center		

Cyclone Thane hit the Tamil Nadu coast in December 2011 and destroyed houses, boats, standing crops, livestock, and livelihoods. As per government sources, the cyclone killed 35 people. The storm clocked wind speeds up to 135 km/h (83 mph) and tidal surges reaching 1.5 m. Cyclonic Storm Nilam (October 2012) was the deadliest tropical cyclonic storm surge. A surge of about 1–1.5 m over the astronomical tide inundated low-lying areas of Chennai, Kancheepuram, Tiruvallur, and Nellore districts. Cyclone Nilam has killed seven people and displaced around 150,000 people in India and Sri Lanka. The Deep Depression occurred in the Bay of Bengal in November 2015. The storm made landfall near Puducherry with peak winds of 55 km/h. It brought heavy rainfall, resulting in extensive flooding and killing 71 people in Tamil Nadu. Very Severe Cyclonic Storm Vardah (December 2016) hit northern Tamil Nadu, uprooting trees and big broken branches blocking the roads, damaging compound walls and vehicles under fallen trees, and causing power cuts. Chennai's vegetation cover considerably decreased as the cyclone uprooted thousands of trees. The major affected areas were the north coastal areas of Chennai, Tiruvallur, and Kancheepuram districts in Tamil Nadu. A maximum gale wind of about 100–110 km/h, gusting to 125 km/h, has been reported in these districts. At landfall, the

maximum storm surge of about 1 m inundated low-lying areas of Chennai, Thiruvallur districts of Tamil Nadu, and Nellore districts of Andhra Pradesh.

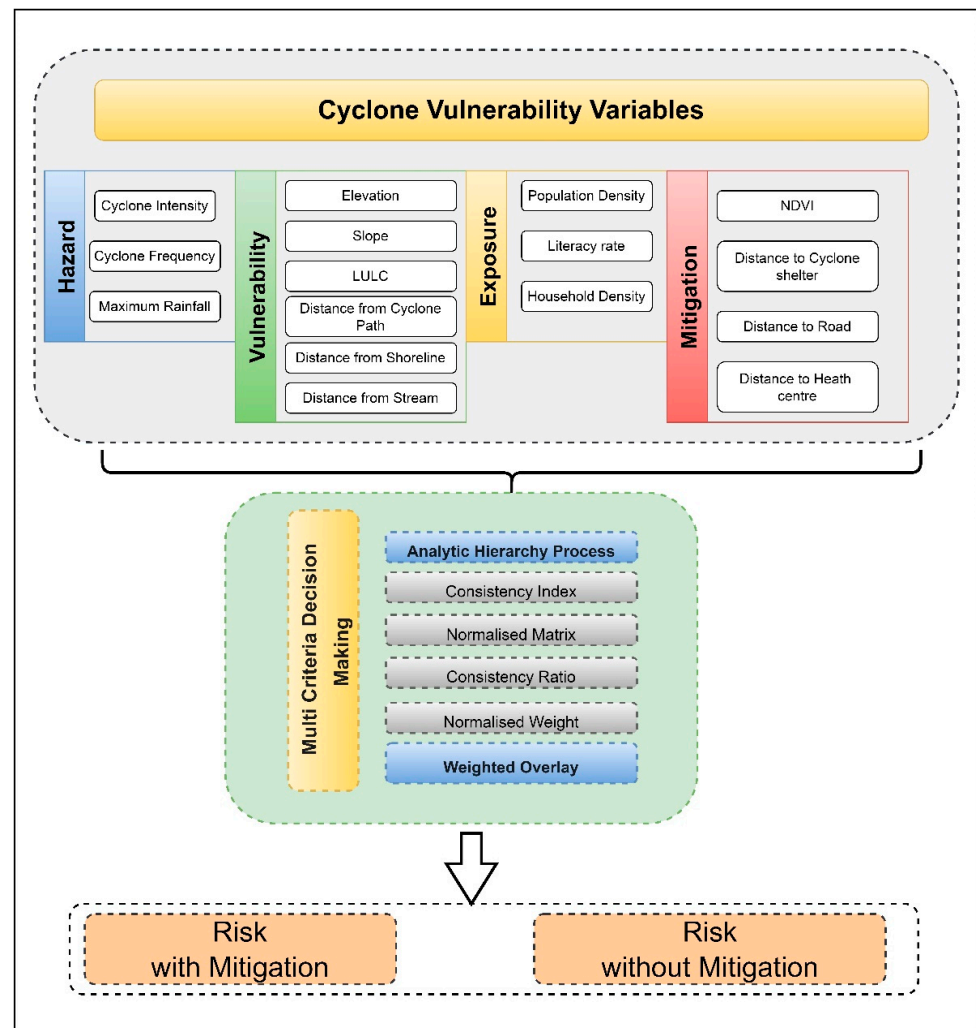
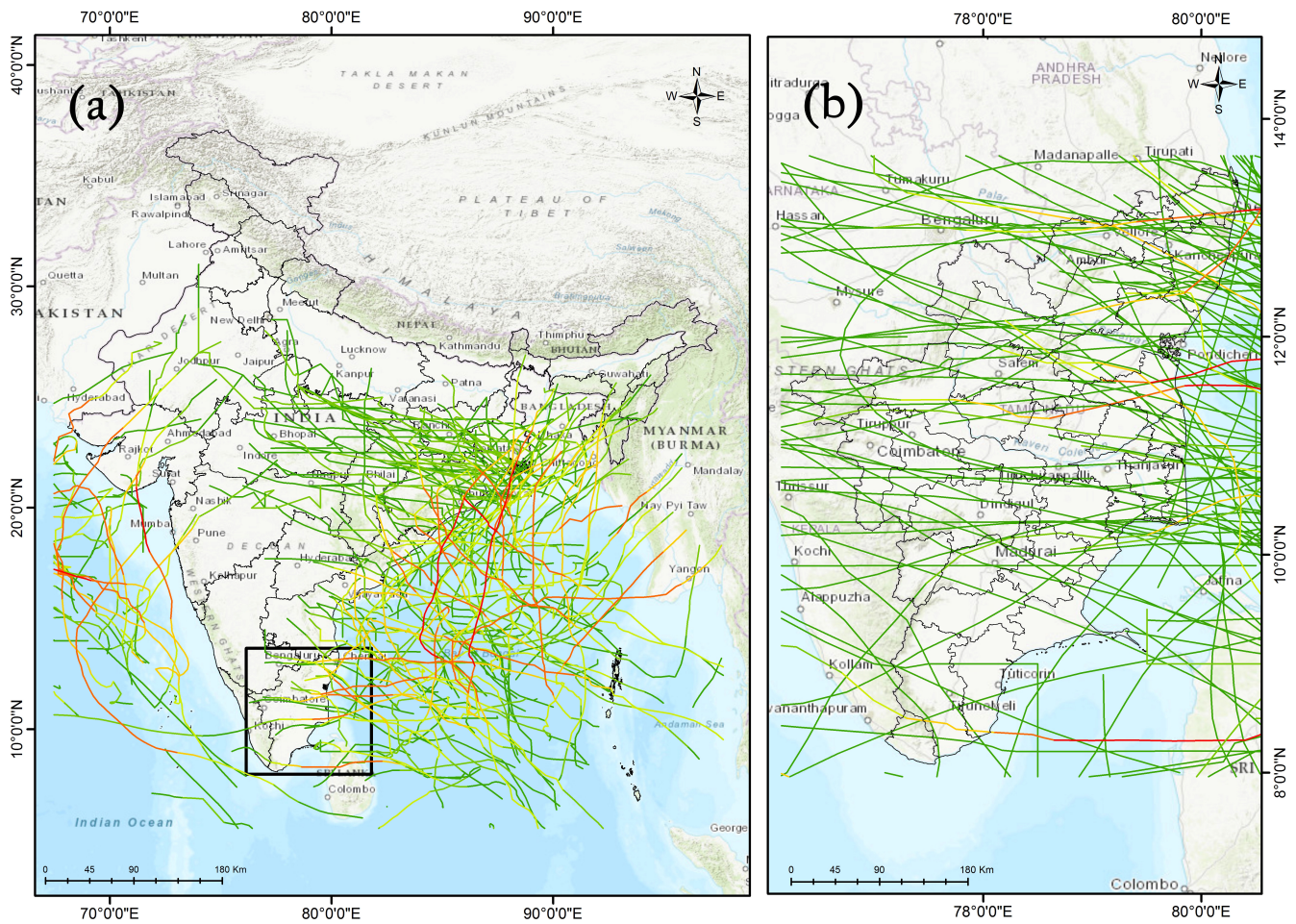


Figure 2. Shows the detailed methodology flow chart for the study.

Cyclone Ockhi (December 2017) caused the deaths or disappearance of over 350 people and injured over 200, affecting many fishermen in southern Kerala and Tamil Nadu. A storm surge of about 1 m above astronomical tides inundated low-lying areas. Cyclone Gaja (November 2018) made landfall in South India at Vedaranyam, Tamil Nadu. At the time of the cyclone’s landfall, speeds of 100–120 km/h were experienced. Losses and damage due to the impact of the cyclone were very high. The reported deaths accounted for 52 people, and 259 people were injured. Almost five lakh people are directly affected, and a storm surge of about 1.0 m above the astronomical tide inundated low-lying areas of Nagapattinam, Thanjavur, Pudukkottai, and Ramanathapuram districts of Tamil Nadu and Karaikal district in Puducherry at the time of landfall. Severe Cyclonic Storm Mandous (December 2022) was the third cyclonic storm and most intense tropical cyclone of the 2022 North Indian Ocean cyclone season. It attained a wind speed of 105 km/h and strengthened into a Severe Cyclonic Storm. About 180 residences were damaged in rain-related incidents.



Cyclone Classification

- Low Pressure Area
- Depression
- Deep Depression
- Cyclonic Storm
- Severe Cyclonic Storm
- Very Severe Cyclonic Storm

Figure 3. (a) Major intense cyclones crossed in India; and (b) All cyclonic storms crossed in Tamil Nadu between 1980 and 2021.

2.4. Methodology

Cyclones represent a natural phenomenon that necessitates the utilization of meteorological data to evaluate their potential impact. However, additional variables may also contribute to the risk associated with these events. A range of variables were gathered from previous literature to evaluate the possible risks posed by cyclones. These factors were subsequently plotted through GIS technology and statistical analysis. The criteria should be relevant, understandable, and justify the actual circumstances. The present investigation involved preparing 16 thematic layers associated with vulnerability, hazards, exposure, and risk mitigation capacity. In this study, the factors contributing to cyclone occurrences were selected based on existing literature, published research, geographic location, and personal findings conducted in the study area. These factors were chosen based on their relevance and significance in assessing cyclone risks. [30,31,50–52]. The georeferencing process utilized the UTM zone 44 N projection system with a spatial resolution of 30 m.

2.4.1. Factors for Cyclone Hazard Evaluation

Hazards are severe occurrences that harm people, property, and the environment. The potential dangerous effects of tropical cyclones are estimated using historical records

and literature. The hazard probability is computed based on the severity, location, timing, intensity, and frequency [50]. For this study, cyclone intensity, cyclone frequency, and maximum rainfall were chosen for hazard evaluation (Figure 4).

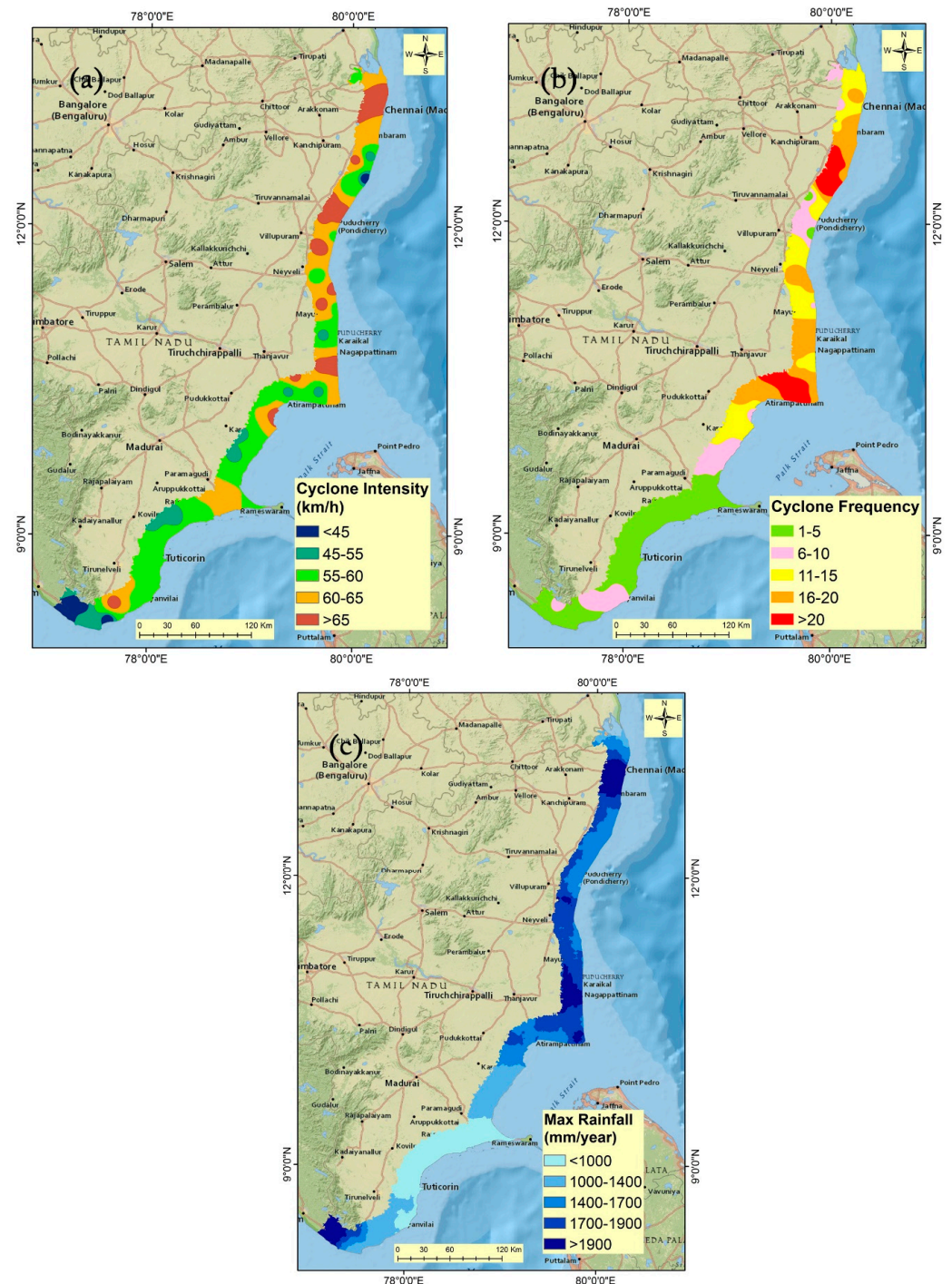


Figure 4. Variables used to calculate Hazard. (a) Cyclone intensity, (b) cyclone frequency, and (c) maximum rainfall.

The intensity of a cyclone directly impacts the magnitude of the storm surge, precipitation levels, wind velocity, and the likelihood of harm to infrastructure and assets. Regions with a higher susceptibility to cyclones, such as coastal areas characterized by low-lying terrain, inadequate infrastructure, and a dense population, are expected to encounter more severe consequences from cyclones of greater magnitude [53,54]. The term

"intensity" pertains to the highest attainable wind velocity that a cyclone can produce. The greater the intensity of a cyclone, the more potential it has for causing destruction. It is imperative for communities and infrastructure situated in regions with a probability of cyclones to consider the possibility of severe storms with high intensity [55]. Cyclone frequency is the number of cyclones that occur in a region over time. It is an important metric in cyclone vulnerability studies as it helps to evaluate the likelihood and frequency of cyclones affecting a specific location. To determine the average frequency of cyclones per year, the total number of cyclones occurring in a region is divided by the duration of the time interval considered [56]. The cyclone intensity and frequency are obtained from the publicly available IBTrACS and IMD datasets. The maximum rainfall parameter holds significant importance in assessing the potential impact of a cyclone in the context of weather-related events. Cyclonic weather events yield extensive precipitation, which may lead to flooding. The maximum rainfall parameter is utilized by researchers investigating cyclone vulnerability to comprehend the impact of cyclones on various regions and to evaluate the potential danger to communities and infrastructure [57]. The study of rainfall in the context of cyclone vulnerability is of great importance. This includes an investigation into the consequences of intense rainfall during cyclones on areas that are susceptible to such incidents, an assessment of the efficacy of early warning systems and measures for flood control, and an analysis of the contribution of vegetation in improving the impacts of heavy rainfall [58]. The maximum average rainfall was collected from 1980–2021 from the IMD dataset.

2.4.2. Factors for Cyclone Vulnerability Evaluation

The degree of vulnerability is the degree of loss to the element at risk as a result of the hazard's occurrence. Distance from the cyclone path, shoreline, and stream, elevation, slope, and LULC are variables for vulnerability mapping (Figure 5). The distance of a region from the path of a cyclone is directly proportional to its probability of causing damage and devastation due to the effects of strong winds, storm surges, and intense precipitation. Typically, regions within a 100-km radius of the cyclone's center are at greater risk of damage. The distance of a region from the path of a cyclonic system can be a crucial determinant in assessing its susceptibility to cyclones. Regions near the anticipated trajectory of a cyclonic storm are typically more susceptible to encountering powerful gusts, surges of water, and extensive precipitation throughout the occurrence [59]. Coastal communities are at a higher risk of encountering erosion and harm to their infrastructure and assets after a cyclonic disruption. Moreover, communities dependent on fishing and other marine-related activities as their source of income may also face adverse consequences due to the damage caused to boats and fishing equipment during a cyclone [60]. The cyclone path is collected from the IBTrACS and IMD datasets, as shown in Table 1.

The shoreline is downloaded from the NOAA Global Self-consistent Hierarchical High-Resolution Shorelines (GSHHS) data. The stream network is downloaded from the OSM data. The study employs the Euclidean distance tool to determine the proximity of the shoreline and stream. In which up to 25 km inland is calculated in the study area. Areas close to streams might have greater vulnerability to flooding and storm surges during cyclonic events [61]. In this study, SRTM DEM, downloaded from the USGS, has been utilized. It is open-access data with a spatial resolution of 30 m. Higher elevations are less susceptible to cyclones, and vice versa. Slope is derived from the DEM data, wherein steep hills are less likely to flood, while low slopes indicate greater risks [62].

LULC analysis is crucial to aiding environmental stability. Inappropriate growth and its impact on natural ecosystems have become crucial for decision-makers and conservationists [63,64]. Landsat 8 is used to generate the LULC map for 2020. The LULC has been classified into five classes: settlement, waterbody, barren land, forest, and agriculture, using the Random Forest algorithm in GEE (Figure 5f). Higher household density may increase the likelihood of damage and fatalities in cyclone-prone locations. High housing densities may also make it more challenging to evacuate residents during a cyclone. Providing

adequate transportation to rapidly and safely evacuate everyone can be difficult, as many people live in isolated locations [65].

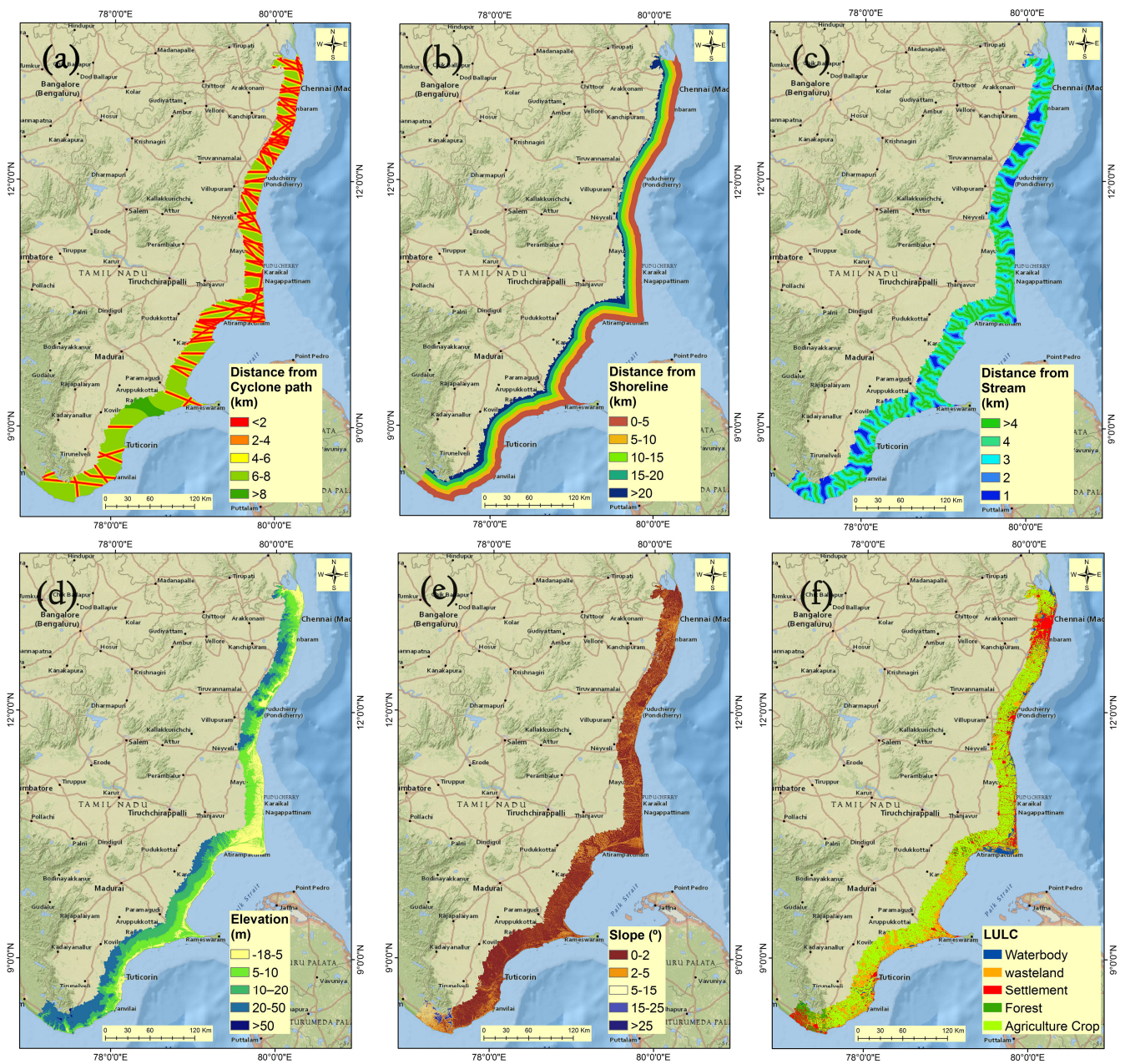


Figure 5. Variables used to calculate Vulnerability. (a) Distance from cyclone path, (b) distance from Shoreline, (c) distance from Stream, (d) elevation, (e) slope, and (f) LULC.

2.4.3. Factors for Cyclone Exposure Evaluation

The inclusion of physical and geographic components within the exposure dimensions of risk is a crucial aspect to consider. This study considers population density, literacy rate, and household density as exposure indicators (Figure 6). The population density in a region can heighten its susceptibility to cyclones due to the concentration of individuals within a limited space. This can pose challenges regarding evacuation and exacerbate the risk of fatalities and harm to infrastructure. Providing sufficient protection for all residents in densely populated areas may be challenging due to the limited space available for cyclone shelters or evacuation centers. Furthermore, densely populated urban regions tend to possess more structures and physical systems, rendering them more susceptible to

destruction from strong winds and inundation [66]. The literacy rate refers to the proportion of individuals who possess the ability to read and write and reside in cyclone-prone areas. Since education and literacy are important for promoting awareness and comprehension of the risks of natural disasters like cyclones, localities with higher literacy rates typically have stronger disaster preparedness and response mechanisms. However, vulnerability to cyclones also depends on several other variables, including infrastructure, access to information, and poverty [8]. Thus, the population density, literacy rate, and household density data are utilized from NASA's SEDAC data.

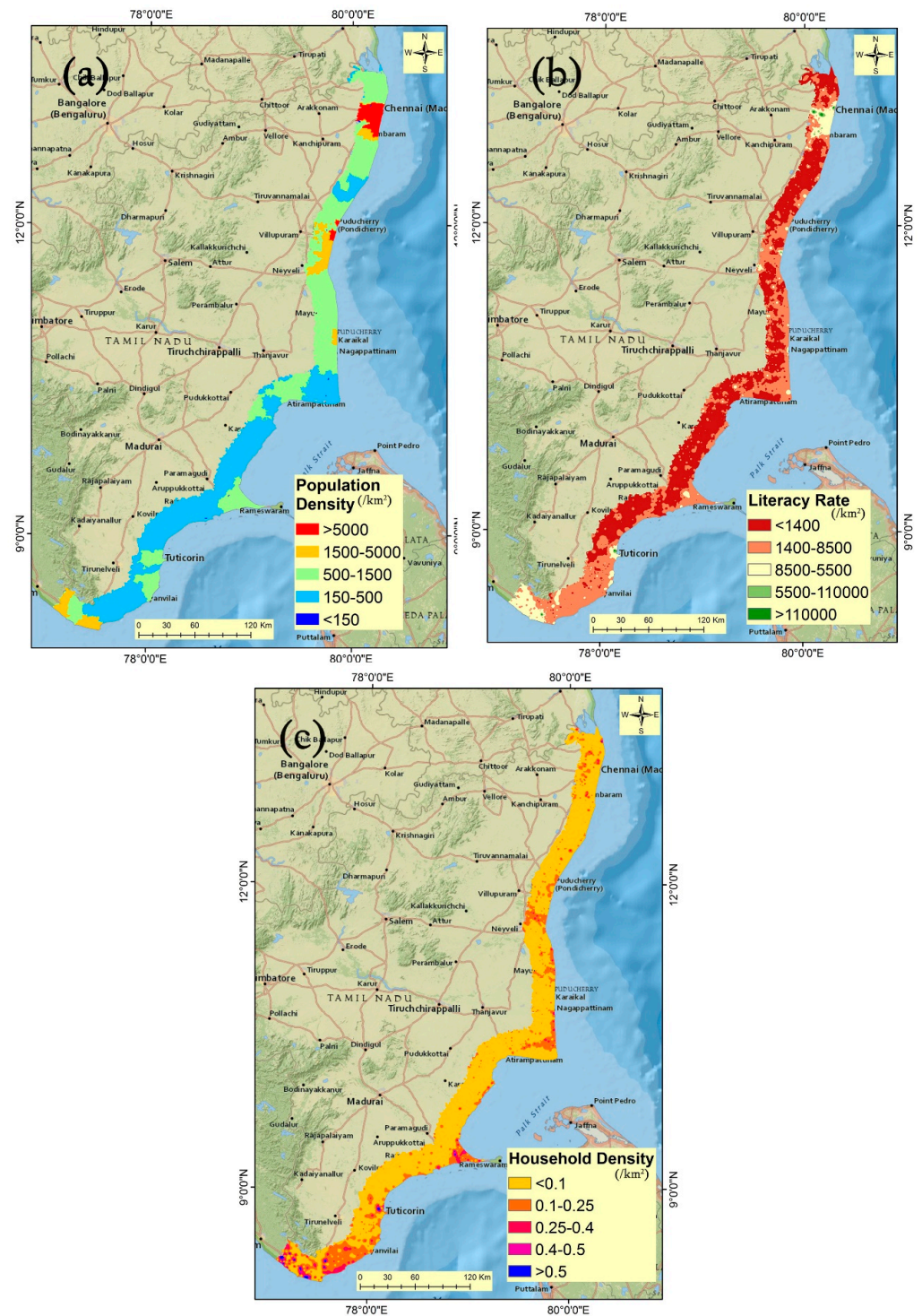


Figure 6. Variables used to calculate exposure. (a) Population density, (b) literacy rate, and (c) household density.

2.4.4. Factors for Cyclone Mitigation Evaluation

Mitigation of coastal hazards can be achieved through three primary strategies: protection, accommodation, and retreat. These approaches encompass both structural and non-structural measures. Structural measures pertain to implementing physical infrastructure, whereas non-structural measures refer to enforcing regulations and disseminating awareness campaigns [67]. The present study incorporates various factors, including proximity to shelters, health centers, roads, and NDVI, in mitigating tropical cyclone hazards (Figure 7).

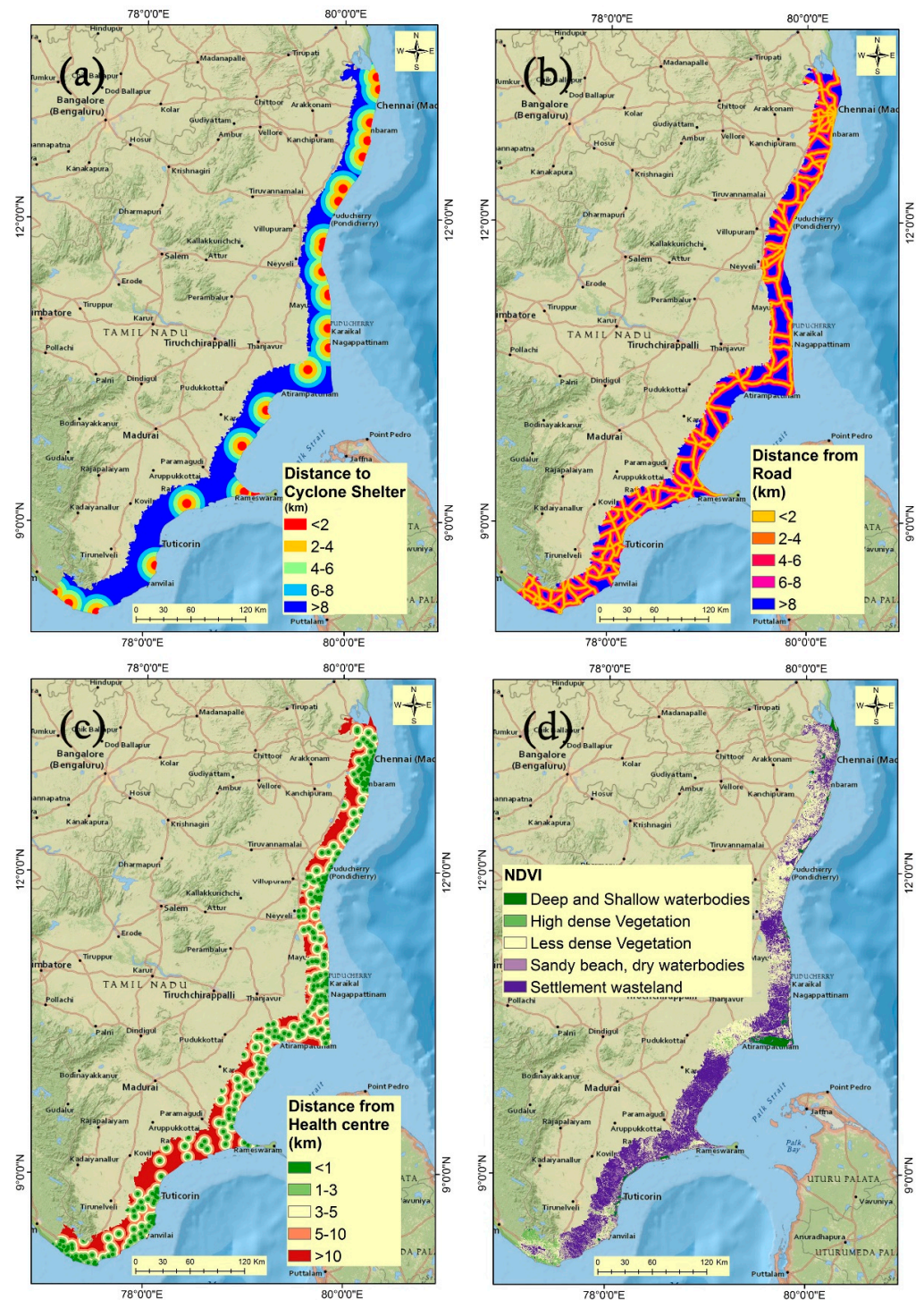


Figure 7. Variables used to calculate mitigation. (a) Distance to the cyclone shelter, (b) distance from the road, (c) distance from the health center, and (d) NDVI.

The proximity of a cyclone shelter can significantly impact one's susceptibility to a cyclone. Cyclone shelters have been specially designed to provide temporary protection for individuals residing in coastal regions susceptible to a cyclone's impact. The shelters are constructed to endure strong winds and flooding and are fitted with essential emergency provisions, including food, drinking water, and medical equipment. It is generally advised that individuals residing in regions susceptible to cyclones have access to a cyclone shelter located reasonably close, typically within a few kilometers [34]. The proximity of the health center can significantly influence a community's susceptibility to the consequences of a cyclone. During a cyclone, the availability of medical assistance can be crucial for individuals who require urgent and essential medical care. In instances where a community is situated quite a distance from a healthcare facility, the response of medical personnel may be impeded, posing a challenge to providing timely and effective medical attention. Furthermore, the occurrence of a cyclone has the potential to cause transportation disruptions or complete termination, thereby posing a challenge for individuals to access a nearby health center [68]. The proximity to the cyclone shelter and health center is digitally extracted from the Google Earth software. Distance from roads significantly influences the cyclone vulnerability index, given its potential impact on evacuation and emergency response operations. In the event of a cyclone, evacuating individuals or transporting resources and supplies may prove challenging in regions situated at a considerable distance from a roadway or possessing inadequate road infrastructure [69]. The distance from the road is extracted from the OpenStreetMap data.

NDVI is a widely employed remote sensing methodology to quantify and monitor vegetation's health. In the context of cyclones, regions characterized by low vegetation cover and density exhibit greater susceptibility to the hazardous effects of cyclones, including soil erosion, landslides, and flooding. The presence of vegetation is a natural impediment, decreasing the velocity of wind and water and mitigating their capacity to erode. Consequently, regions exhibiting elevated NDVI values may exhibit comparatively lower susceptibility to the effects of cyclonic disturbances when contrasted with regions characterized by diminished NDVI values [70,71]. The NDVI is created from Landsat 8 data for the year 2020 using GEE.

The AHP technique was proposed by Saaty [72–74]. It helps decision-makers solve complex spatial problems related to environmental issues. Multiple parameters have been considered for determining cyclone vulnerability. The methodology comprises the following main steps: (1) definition of the vulnerability matrix; (2) definition and scoring of vulnerability classes; (3) assignment of weights to vulnerability factors; (4) aggregation of vulnerability factors; (5) normalization and classification of vulnerability values; (6) construction of vulnerability maps. Thus, the weight and rank of each factor are calculated by creating the pairwise comparison matrix, by which the individual weights of the layers are determined.

3. Results

The final AHP weights for each factor and their respective classes, deduced as shown in Table 2, are calculated to derive the final cyclone risk map for the Tamil Nadu coast. The pairwise comparison matrix is used to generate each component of the cyclone risk index, which is then totaled to 100%. In the Hazard component, cyclone intensity is one of the main factors with a weight of 0.63. With a weight of 0.33, distance from the cyclone path is an essential factor in vulnerability. Population density is a key factor in the exposure component, with a weight of 0.49. Distance from cyclone shelter is one of the most critical factors in mitigation, with a weight of 0.43. The weights of each class in the factors are also totaled to 100%. Then the weights for each class are multiplied with those of the factors in each component to obtain the final cyclone risk map. Locations with a higher rating are more susceptible to cyclones, and vice versa. Classifying the results into a range of distinct vulnerability maps is essential. The natural break categorization method classifies their forecasts' outcomes into five categories: very low, low, moderate, high, and very high. By

applying Jenks optimization, also known as natural break classification, one may determine the optimal value effect of various classes. This categorization approach reduces the average difference between classes while increasing the gap within each class [75]. Consequently, the strategy minimizes inequality within classes while concurrently increasing inequality across groups [76]. The percentage area of hazards, vulnerability, exposure, mitigation, and cyclone risk is shown in Figure 8.

Table 2. Ratings and weights based on AHP for cyclone vulnerability.

Components	Factors	Class	AHP Weight for Classes	AHP Weight for Factors
Hazard	Cyclone Intensity (km/h)	<45	0.12	0.63
		45–55	0.15	
		55–60	0.19	
		60–65	0.24	
		>65	0.31	
	Cyclone Frequency	1–5	0.12	0.26
		6–10	0.13	
		11–15	0.19	
		16–20	0.26	
		>20	0.30	
Maximum Rainfall (mm/yr)	<1000	0.10	0.11	
	1000–1400	0.15		
	1400–1700	0.20		
	1700–1900	0.24		
	>1900	0.31		
Vulnerability	Distance from cyclone path (km)	0–5	0.37	0.33
		5–10	0.24	
		10–15	0.18	
		15–20	0.13	
		>20	0.08	
	Distance from Shoreline (km)	1	0.32	0.24
		2	0.23	
		3	0.20	
		4	0.15	
		>4	0.10	
Distance from stream (km)	>4	0.12	0.17	
	4	0.15		
	3	0.19		
	2	0.23		
	1	0.31		
Elevation (m)	0–5	0.32	0.14	
	5–10	0.24		
	10–20	0.19		
	20–50	0.15		
	>50	0.10		

Table 2. Cont.

Components	Factors	Class	AHP Weight for Classes	AHP Weight for Factors
Exposure	Slope (°)	0–2	0.29	0.07
		2–5	0.26	
		5–15	0.21	
		15–25	0.14	
		>25	0.10	
	LULC	Waterbody	0.09	0.05
		Forest	0.16	
		Agriculture	0.26	
		Settlement	0.32	
		wasteland	0.17	
Exposure	Population density (/km ²)	>5000	0.32	0.49
		1500–5000	0.29	
		500–1500	0.18	
		150–500	0.12	
		<150	0.09	
	Literacy rate (/km ²)	<1400	0.32	0.31
		1400–8500	0.29	
		8500–55000	0.18	
		5500–110,000	0.12	
		>110,000	0.09	
Household density (/km ²)	<0.1	0.10	0.20	
	0.1–0.25	0.15		
	0.25–0.4	0.20		
	0.4–0.5	0.23		
	>0.5	0.32		
Mitigation	Distance from cyclone shelter (km)	<2	0.10	0.43
		2–4	0.13	
		4–6	0.20	
		6–8	0.26	
		>8	0.31	
	Distance from Road (km)	<2	0.12	0.26
		2–4	0.15	
		4–6	0.19	
		6–8	0.24	
		>8	0.30	
Distance to the health center (km)	<1	0.08	0.20	
	1–3	0.12		
	3–5	0.17		
	5–10	0.25		
	>10	0.38		

Table 2. Cont.

Components	Factors	Class	AHP Weight for Classes	AHP Weight for Factors
	NDVI	Deep and Shallow waterbodies	0.08	0.11
		Settlement wasteland	0.12	
		Sandy Beach, dry waterbodies	0.16	
		Less dense Vegetation	0.25	
		High dense Vegetation	0.39	

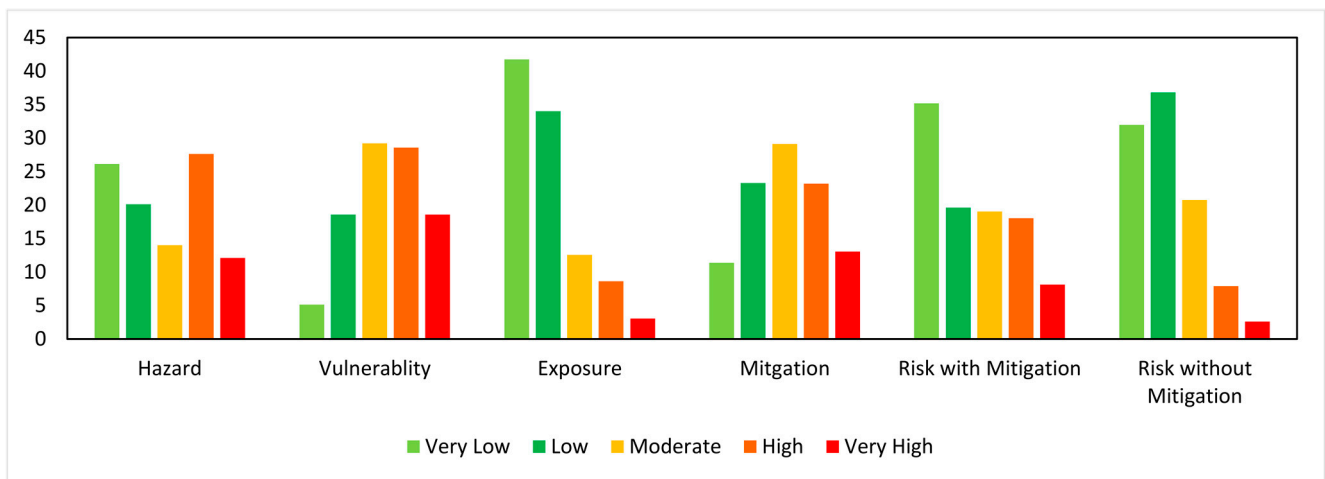


Figure 8. Percentage area of cyclone index.

3.1. Hazard

A hazard map (Figure 9a) for cyclone vulnerability typically includes cyclone intensity, cyclone frequency, and maximum rainfall for mapping hazards. In this study, cyclone intensity ranges from <45 to >65 km/h; zone 1 and zone 2 have concentrations of extremely intense cyclones, with Chennai and Cuddalore being particularly vulnerable. In zone 3, the Nagapattinam region has clusters of high intensity. In zone 3, the Rameshwaram region has a cluster of cyclones that occurred in 1964, and zones 3, 4, and 5 are generally low intensity. The cyclone frequency plays a crucial role in identifying areas at a higher risk of experiencing recurrent cyclones, leading to substantial damage and the loss of human lives. The frequency of cyclones ranges from 1 to >20, with the southern regions of Chennai and Nagapattinam having the highest frequency. The connection between rainfall and the landfall of tropical cyclones leads to inundation and agricultural loss. From the spatial map, zones 1, 2, and 5 have high rainfall regions with maximum precipitation ranging from 1000 to >1900 mm. Zone 4 falls in a moderate rainfall region, and zone 3 generally receives less precipitation. The technique of kernel density estimation was employed to generate a spatial layer. Considering these three parameters, the hazard is calculated, and the spatial distribution reveals that 12.10% of the area is classified as a very high zone and 27.62% as a high zone. These zones are located predominantly in zones 1 and 2. The moderate zone encompasses 14.02% of the study area and is located primarily in the southern part of zone 2 and the northern portion of zone 3. The low and very low vulnerable zones comprise 20.01% and 26.14% of the study area and are dispersed throughout all zones.

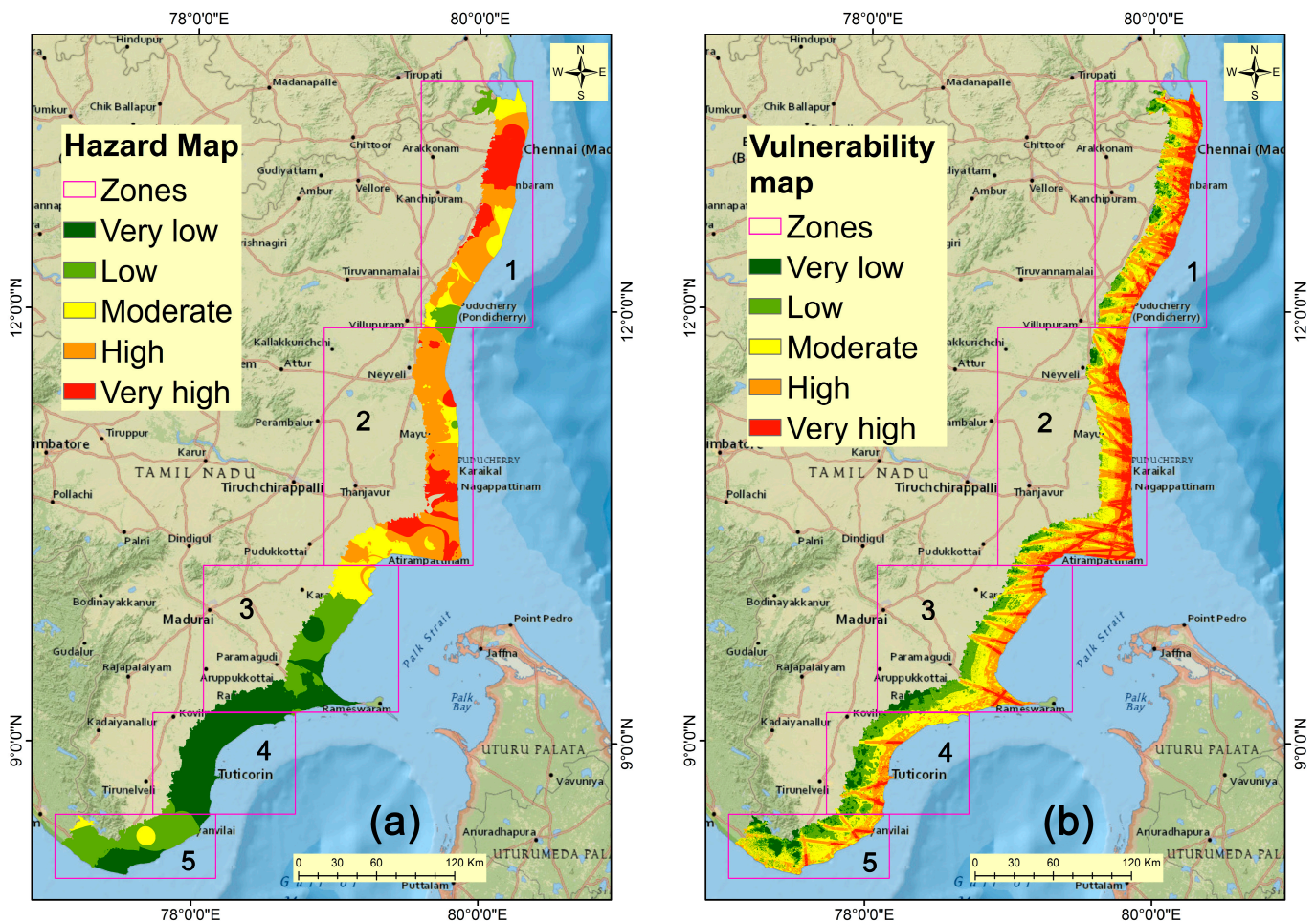


Figure 9. Resultant maps associated with cyclones. (a) Hazard map and (b) vulnerability map.

3.2. Vulnerability

When mapping vulnerability, several factors are considered, including distance to the cyclone path, distance from the shoreline, elevation, slope, and LULC. Figure 9b represents the exposure map. The cyclone path is used to evaluate the vulnerability to tropical cyclones, ranging from 2 to >8 km; the concentrations are higher in zones 1 and 2. Zone 3 is moderate because the number of cyclones is minimal, while zones 4 and 5 are low. The distance from the shoreline ranges from 0 to 20 km, where the closeness to the shore is more susceptible to the effects of tropical cyclones. Most coastal communities have densely populated regions near the shore, including Chennai, Pondicherry, Cuddalore, Nagapattinam, Thoothukudi, and Kanyakumari. Tropical cyclones pose a significant threat to areas with low elevations and slopes. The elevation ranges from 0 to 50 m, and the slope gradients from 0 to 25°. Most coastal cities fall within 0 to 10 meters of elevation and 0 to 5° of slope. The beaches in Kanyakumari exhibit a greater degree of variance in elevation and slope as they are characterized by rocky outcrops and isolated stretches of sand. Whereas Chennai, Cuddalore, and Nagapattinam regions have minimal elevation and slope. LULC is a valuable exposure and indicator for tropical cyclone vulnerability, and the LULC map reveals that coastal cities have concentrations of settlement. In zone 2, the Kaveri Delta has more agricultural land. Pulicat Lake and Point Calimere are large bodies of water and wasteland visible throughout the study area. The mangrove forests of the Pichavaram region near the coast and the upland region in zone 5 are notable for their forest cover. The analysis of spatial distribution in vulnerability reveals that the very high (18.56%) and high (28.56%) classes are prevalent in zones 1 and 2. The moderate (29.19%) vulnerability class

is widespread in the study area, whereas the low (18.55%) and very low (5.12%) classes are primarily located in zones 3, 4, and 5.

3.3. Exposure

Exposure denotes the extent to which individuals and resources are susceptible to a specific cyclonic calamity. Figure 10a represents the exposure map associated with the physical, environmental, and socio-economic conditions of both populations and assets. In this study, the exposure parameters considered are Population density, literacy rate, and Household density. Population density ranges between >5000 and <150. Most regions have a moderate population density, whereas Cuddalore and Kanyakumari have a high population density, and Chennai and Pondicherry have a very high population density. Literate people are more aware of cyclones' effects, and the literacy rate ranges from 1400 to >110,000. One or two locations in Thoothukudi, Kanyakumari, and Chennai have a high literacy rate. The majority of studies show a low literacy rate. In contrast to their population densities, Chennai and Kanyakumari have a high literacy rate. Due to the high household density, the area is highly susceptible to tropical cyclones. The household density in this study ranges from <0.1 to >0.5. The important cities along the coasts have a very high density, while most regions have a moderate density. The spatial distribution of exposure reveals that 3.04% of the area is classified as a very high exposure zone and 8.64% as a high exposure zone. The moderate zone encompasses 12.54%. Low and very low exposure zones comprise 34% and 41.7% of the study area, respectively, and are dispersed throughout all zones.

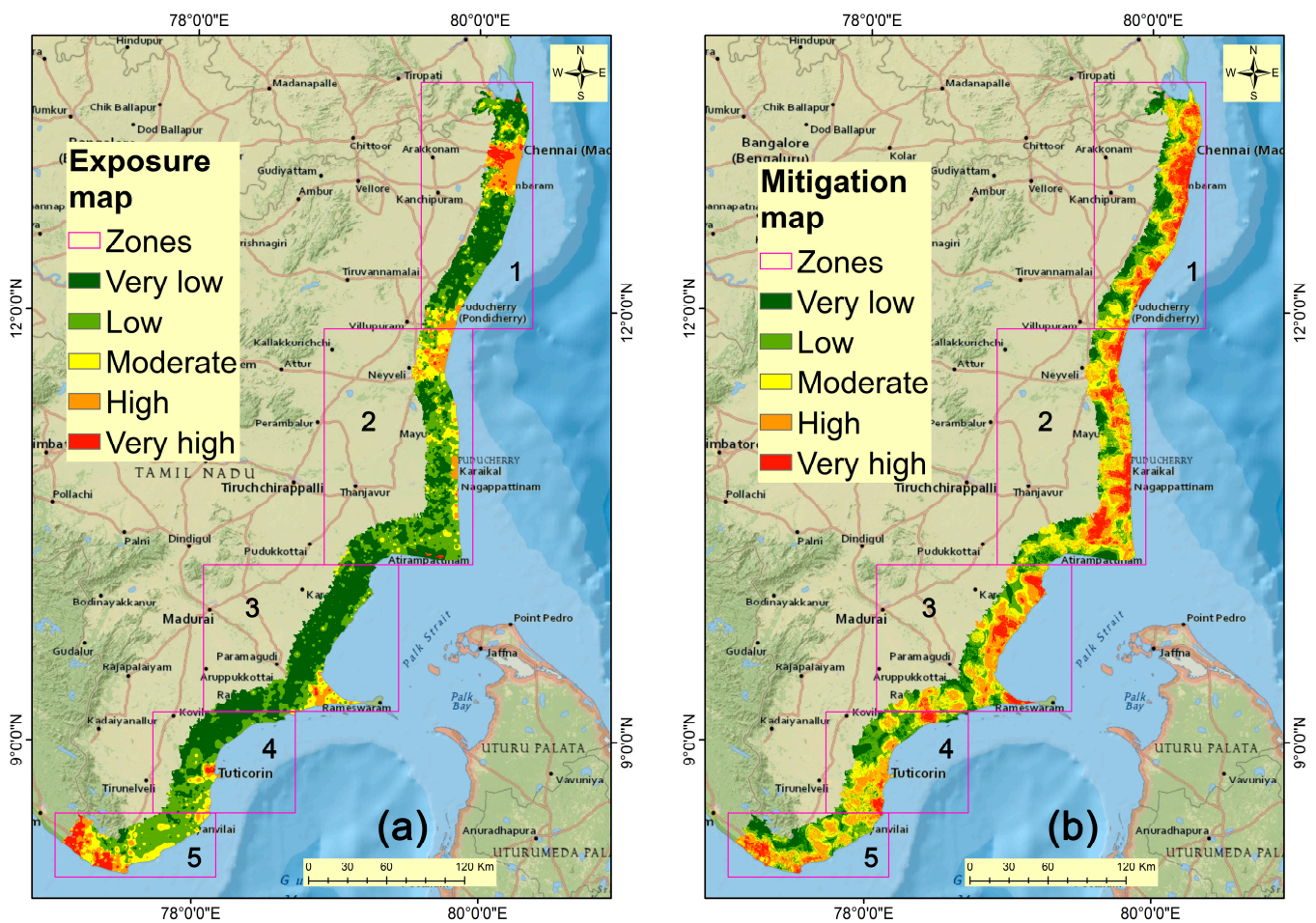


Figure 10. Resultant maps associated with cyclones. (a) Exposure map and (b) Mitigation map.

3.4. Mitigation

Mitigation (Figure 10b) is the measure taken to reduce and protect the impact of cyclones on vulnerable populations and infrastructure. In this study, distance from the cyclone shelter, Distance from the road, Distance to the health center, and NDVI are considered. The distance from the cyclone shelter and distance from roads ranges from <2 to >8 km. The coastal cities, especially those in zones 1 and 2, have the greatest number of shelters and the best road connections, and the majority of the study area is considered to be safe in terms of both shelter availability and improved road connectivity. The distance to the health center ranges from <1 to >10 km. Even though local health facilities also provide emergency care before a cyclone's landfall, the number of centers near the coast is low throughout the study area. During cyclone occurrences, NDVI is seen as a protective measure because of its ability to lessen the impact of wind and storm surges on coastal areas. NDVI is classified based on the index values in this study as deep and shallow waterbodies, settlements, wasteland, sandy beaches, dry water bodies, less dense vegetation, and high dense vegetation. Most of the region is covered by waterbodies, Settlement wasteland, Sandy Beach, and dry water bodies. High-density vegetation is seen near the Pichavaram mangrove and Deep and Shallow waterbodies in Pulicat Lake and Point Calimere. The spatial extent of mitigation reveals that 13.07% of the study region comes under the very high hazard zones; 23.17% are high; 29.11% are moderate; 23.27% and 11.36% are low and very low zones, respectively.

3.5. Risk

The risk map is used to evaluate the region prone to cyclones, in which the study considers two scenarios, i.e., with mitigation and without mitigation. The risk map with mitigation (Figure 11a) shows the ability of the community resilience in the study, whereas the risk map without mitigation (Figure 11b) shows the effect of the cyclonic hazard on the coastal districts of Tamil Nadu. Various literatures have widely used the United Nations proposed definition of the risk method [77] for evaluating the vulnerability of tropical cyclones [30,78,79]. According to the principle of risk, the risk assessment model considers hazards, vulnerability, exposure, and mitigation, and the cyclone risk index was computed as follows:

$$R = \left[\frac{H \times V \times E}{M} \right] \quad (1)$$

where R is the risk, H is the hazard, V is a vulnerability, E is the risk exposure, and M is Mitigation.

The risk assessment without considering mitigation measures indicates that a significant portion of the study area falls under the high-risk categories, with 8.12% in the very high-risk category and 18.03% in the high-risk category. Moderate-risk areas cover 19.02% of the study area, while the very low-risk and low-risk categories comprise 19.61% and 35.19%, respectively. However, when mitigation measures are considered, the risk map shows a notable reduction in the high-risk categories, with only 2.59% in the very high-risk category and 7.59% in the high-risk category. The moderate-risk areas cover nearly 20.33% of the study area, while the very low-risk and low-risk categories cover 37.50% and 31.98%, respectively. Most regions in zone 1 and zone 2 are at significant risk from cyclones, including Chennai, Cuddalore, Nagapattinam, and the Cauvery Delta areas. The comparison of the two risk maps reveals that the mitigation parameters reduce their risk. The results were consistent with the degree of vulnerability and hazard, namely: distance to shore, low elevation, steep slope, dense population, cyclone intensity, and maximum rainfall. Including mitigation measures has led to a significant reduction in the high-risk categories in zone 1 and zone 2, indicating that such measures positively impact reducing the vulnerability of the study area to cyclone hazards.

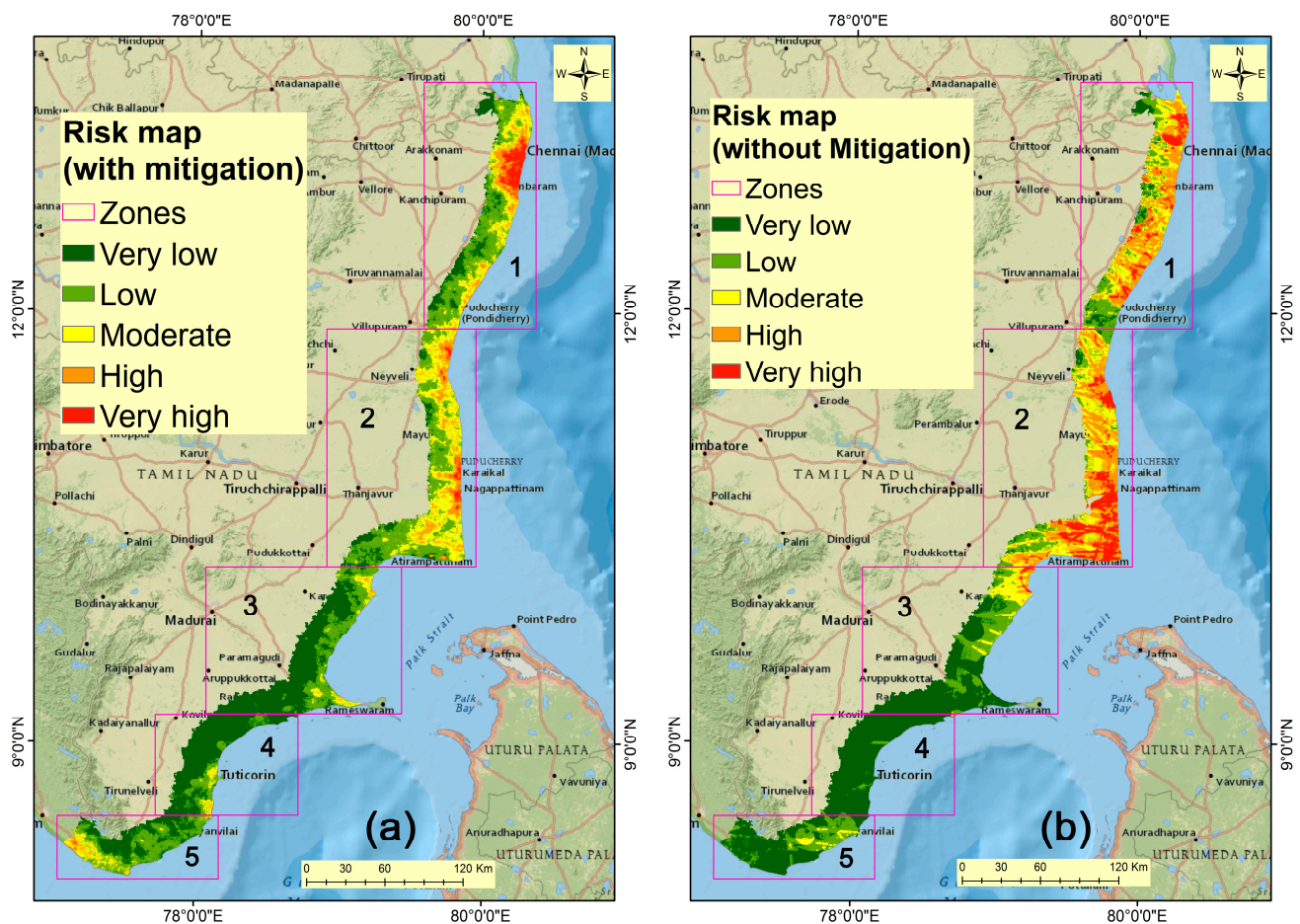


Figure 11. Cyclone risk maps with cyclones. (a) Risk map with mitigation; (b) risk map without mitigation.

4. Validation

The validation of a cyclone risk map using a recently occurring cyclone provides important insights into the accuracy and effectiveness of the map. The validation of cyclone risk maps with actual events will enhance their reliability and utility in decision-making processes related to disaster management. In this research, the evaluation of the cyclone risk map is carried out by comparing it with the impact and damage caused by Cyclone Gaja (Figure 12). The employed methodologies yielded reliable results in validating our risk assessment approach, thereby substantiating the reliability of our data and mapping procedures. The storm intensified into a Severe Cyclonic Storm on 11 November 2018. It made landfall on the Tamil Nadu coast between Nagapattinam and Vedaranyam (10.45° N and 79.8° E) on 16 November 2018 with a maximum wind speed of 70 knots, gusts of about 53.9 knots, and an average rainfall of 22.31 mm. It was observed and classified as a Very Severe Cyclonic Storm. Further, Gaja survived to move into districts of Tamil Nadu such as Nagapattinam, Thanjavur, Thiruvavur, Karaikal, Cuddalore, Trichy, Pudukkottai, Ramanathapuram, and Dindigul [80]. The photographs in Figure 13 depict the aftermath of Cyclone Gaja in the regions of Vedaranyam. Findings suggested that the hazard, vulnerability, exposure, mitigation, and risk without adding mitigation and risk with a mitigation map provide a good estimate of the areas likely to be affected by a cyclone. Furthermore, the risk outcomes verified by comparing them with cyclone events strengthen our confidence in the accuracy of our findings. However, some discrepancies between the map and the actual impact of the cyclone are identified, which can be attributed to factors such as the intensity and track of the cyclone and the accuracy of the input data used for generating the map. One of the most arduous aspects of regional risk assessment is the process of validation. The verification of risk assessment quality is contingent upon the

ability to assess the reliability of the generated risk map through comparison with historical disaster damage data. Unfortunately, damage data are scarce, which means that most risk evaluations presented in the literature cannot be confirmed.

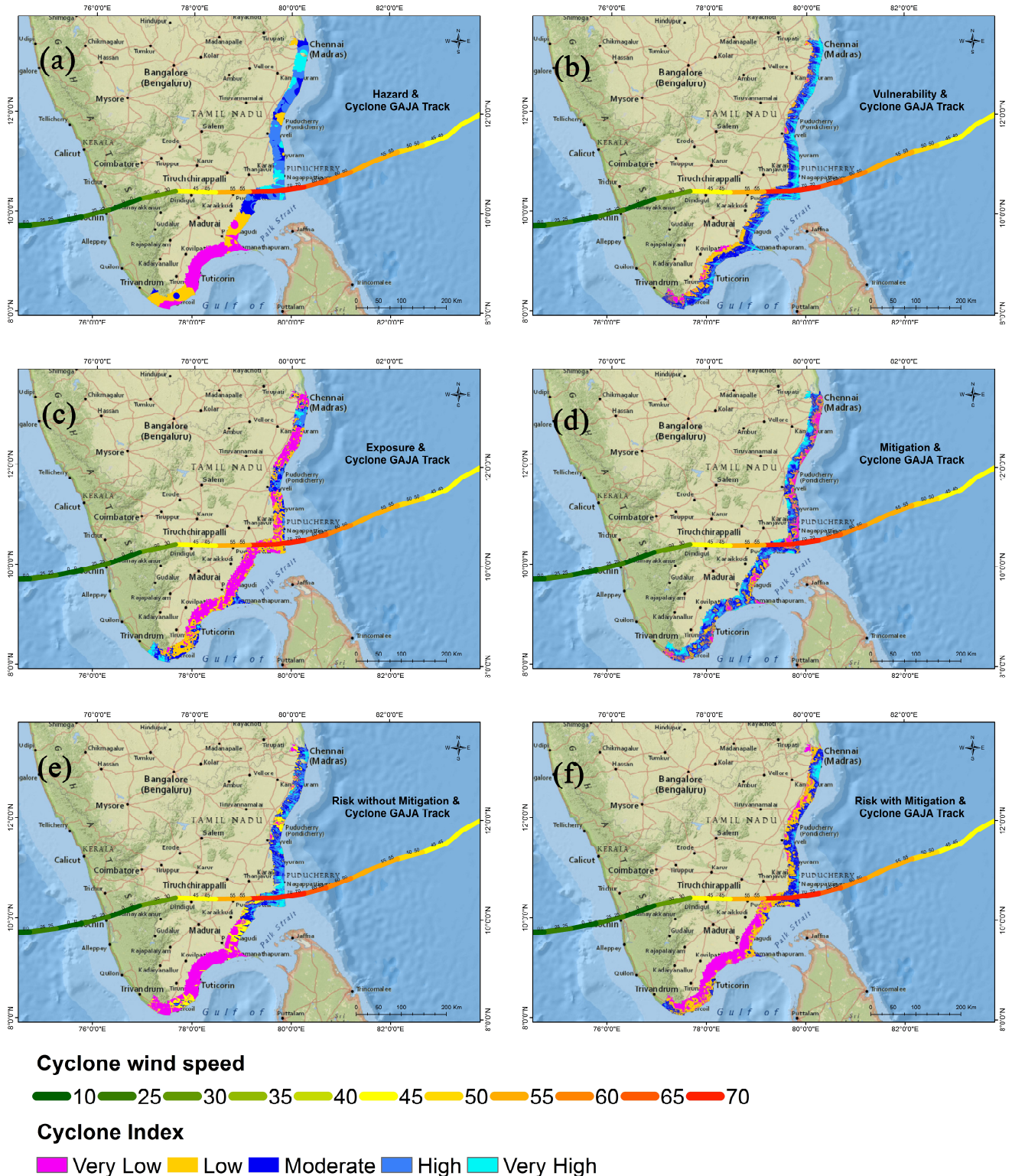


Figure 12. Track of Cyclone Gaja is overlaid with (a) hazard, (b) vulnerability, (c) exposure, (d) mitigation, (e) risk without mitigation, and (f) risk without mitigation.



Figure 13. Field photographs taken aftermath of Cyclone Gaja in the regions of Vedharanyam.

5. Discussion

Cyclones can wreak havoc on coastal communities through heavy rainfall, inundation, landslides, and infrastructure damage. Climate models continue to predict future decreases in global tropical cyclones, projected increases in the intensities of the strongest storms, and increased rainfall rates [81]. When a cyclone makes landfall, it can bring intense winds and heavy rainfall, resulting in widespread inundation and landslides [82]. Flooding and landslides can cause extensive property damage, disrupt livelihoods, and damage vital infrastructure such as roads, bridges, and electricity lines [83]. Apart from the primary impacts of the cyclone, there may also be secondary consequences, such as uprooted trees and crop damage. In addition to further destruction of property, the uprooted trees may block the roads, posing a challenge for emergency personnel to access the affected areas. Crop damage can result in food shortages and farmers' income losses [80].

Tamil Nadu's coast has different geological coastlines, such as alluvial coastlines from Pulicat to Vedaranyam and Mandapam. Deltaic Coastline from Mandapam to Kanniyakumari. Sand Dunes Coastline from Kanniyakumari to Nagercoil Barrier Beach [84]. As natural geomorphic barriers, dune ridges shield the hinterland from extreme oceanographic wave run-ups. Wide coastlines and tall dunes are effective wave energy dissipators. Consequently, sand dunes serve as reserves from which powerful surges draw during

extreme events [85]. Sri Lanka acts as a barrier, blocking or weakening the intensity of cyclonic winds and reducing their direct impact on the central Tamil Nadu coast. This geographical positioning can help mitigate the severity of cyclones by providing a natural buffer zone for the coastal communities of central Tamil Nadu. Even in a disaster like the tsunami, the devastation to this region was minimal. In addition, the coastline is a bay formation with little littoral drift activity [86]. The northern region's geographic location makes it vulnerable to various natural hazards, including tropical cyclones, storm surges, and coastal flooding. The Bay of Bengal puts it in the path of many tropical cyclones that form in the region, particularly during the monsoon season from June to September [87,88]. The role of precipitation in cyclone vulnerability is significant for several reasons. Heavy rainfall associated with cyclones can cause extensive damage in vulnerable areas. The amount of precipitation influences the effectiveness of early warning systems and flood control measures. Vegetation also plays a crucial role in mitigating the impact of heavy rainfall. A region's vulnerability to a cyclone depends on multiple variables, such as the intensity and extent of the cyclone, the terrain and infrastructure of the area, and the preparedness and resilience of the local population. Areas outside the direct path of a cyclone can still experience significant consequences, particularly in low-elevation and coastal regions, including intense precipitation and flooding [89].

The Bay of Bengal is more prone to cyclones and depressions than the Arabian Sea and is frequently affected. Gujarat is the most vulnerable state to tropical cyclones originating in the Arabian Sea [90]. Deadly cyclones like Severe Cyclonic Storms mainly originate in the Bay of Bengal due to warm air. Tropical cyclone paths may suddenly deviate during their active period, and most historical cyclone hits occurred during September, October, and November [91,92]. The South Indian Ocean's primary cyclone season is from May–July and September–December, with significant occurrences of storms in April and August based on the historical return period data [93]. The present cyclone prediction models exhibit certain limitations. The predictive capacity of these models is frequently compromised by the insufficient incorporation of oceanic variables, resulting in inaccurate projections of cyclonic intensity. Consequently, the models exhibit limitations in their ability to comprehensively depict the magnitude and severity of cyclones [94]. Using data from a 50-year return period to simulate storm surges, concomitant water levels, and inland inundation, Rao, A.D., et al. [95] conducted a study of the Kalpakkam region in which the extreme water levels were determined by calculating the 50-year return period.

Experiments determined that the region is susceptible to inundation when the pressure deficit reaches or exceeds 66 hPa. The study also found that the peak surge caused horizontal inundation to extend between 1 and 1.5 km inland. According to Saravanan et al. [89], the northern coastal taluks of Tamil Nadu are more vulnerable to cyclones than the southern coastal taluks. The most vulnerable areas were Ponneri, Cheyyur, and Tindivanam taluks, which fell under the very high cyclone vulnerability zone. In contrast, Sirkali, Tharangambadi, Pattukkottai, Peravurani, Rameswaram, Agastheeswaram, Kalkulam, Vilavancode, and Karaikal taluks were the safest regions. Karuppusamy et al. [96] analyzed the socio-economic vulnerability of micro-administrative units along the coastal plains of Tamil Nadu. Household data-based indicators were used to determine the degree of vulnerability, and the indicators were summed up to identify the hot spots of socio-economic vulnerability. The results showed that approximately 60% of the villages in the coastal stretch from Nagapattinam to Puducherry, including major parts of the Cuddalore district, were highly vulnerable to multi-hazard risks. The cyclone risk maps also revealed a noteworthy observation, indicating that the absence of adequate mitigation measures leads to an escalation in cyclone risk. The aforementioned statement elucidates that the regions of Rameshwaram, Tuticorin, Tirunelveli, and Kanyakumari, falling within zones 4 and 5, are classified as low to moderate risk areas in the risk maps with mitigation measures. Conversely, the risk map without mitigation indicates that the majority of these regions are categorized as very low-risk zones. This phenomenon may be attributed to the

higher concentration of settlements in these regions, coupled with the limited availability of cyclone shelters.

Collaboration between the public and government is crucial for developing resilience to natural disasters. This involves identifying potential risks, creating strategies to mitigate them, and implementing preparedness measures to minimize the impact of disasters. The public can contribute by raising awareness on social media, being ready, and following evacuation orders when necessary. The government can participate by providing resources, policies, and funding for disaster risk reduction and preparedness programs [97]. Effective collaboration between the public and government can lead to better disaster management and more resilient communities [98]. To reduce the likelihood of cyclone damage, destruction, and losses, various services and facilities, such as health and civil defense facilities, should be evaluated for preparedness and mitigation methods. Structures like cyclone shelters and hospitals should be built in layers. Mangrove forests and other dense trees can act as barriers that protect coastal settlements from high waves, decrease wind intensity, and reduce the severity of deadly storms. To enhance disaster response and management, facility distribution, coverage, and accessibility should be measured. Schools or other community facilities can be used as cyclone shelters, so they should be appropriate and easily accessible. Hospitals and clinics offering medical treatment should be properly maintained to reduce risks.

6. Conclusions

The research utilized geospatial techniques and the AHP method to assess the hazards, vulnerability, exposure, and risks of cyclones on the Tamil Nadu coast by taking a total of 16 variables into account. Zone 1 and zone 2 are particularly susceptible to cyclonic activity, and these regions encompass significant agricultural and industrial areas. The study also revealed that low-lying areas and coastal urban settlements are at a higher risk of experiencing damage and casualties caused by cyclones, and these areas also have high vulnerability and low capacity for mitigation. Furthermore, the research included the distribution of assets in key sectors such as housing, education, and employment to determine the exposure index, which indicated that the concentration of assets and their proximity to the coastline are closely linked to the level of exposure to cyclone risks. In order to mitigate the risks associated with potential disasters and their dramatic economic and social implications, it is recommended that disaster preparedness plans be implemented in these regions. The outcomes of this study will benefit developing nations in terms of facilitating efficient planning to mitigate the destructive impacts of coastal hazards. Expensive engineering interventions will probably be required to safeguard the highest societal significance. The methodology utilized in this research is broad, rendering it applicable for implementation in numerous coastal regions worldwide. For developing countries like India, the results of this study will be useful for effective planning and to mitigate the devastating effects of coastal hazards. Engineering solutions are likely necessary to protect the most valuable portions of the threatened coastline. The study is sufficiently general that it can be adapted in many other coastal regions worldwide to identify a pathway toward adopting more integrated coastal management approaches.

Limitations are common in research, and this study is no exception. Such limitations include the absence of numerical predictive modeling and event-based studies like the size and speed of tropical cyclones, which have the potential to yield more precise results regarding the relevant timeframe. The enhancement of model results can be effectively achieved by improving the data resolution, which is a crucial constraint. Incorporating climate change as a variable in accounting and using machine learning models for predictive purposes presents a promising avenue for future research. Unmanned aerial vehicles (UAVs), commonly known as drones, have facilitated the acceleration of the assessment process and provided valuable insights for the strategic planning of response activities. UAVs emerged as a viable solution for the efficient and economical acquisition of geospatial data, thereby facilitating the production of accurate and high-resolution cartographic

products. The maps are equipped with pertinent characteristics, such as geographic coordinates and land elevation particulars, which are beneficial in making sensible choices regarding the placement and construction of emergency shelters.

Author Contributions: Conceptualization, Subbarayan Saravanan, Devanantham Abijith, Parthasarathy Kulithalai Shiyam Sundar and Nagireddy Masthan Reddy; methodology, Subbarayan Saravanan and Devanantham Abijith; software, Devanantham Abijith and Parthasarathy Kulithalai Shiyam Sundar; validation, Devanantham Abijith and Parthasarathy Kulithalai Shiyam Sundar; formal analysis, Devanantham Abijith and Parthasarathy Kulithalai Shiyam Sundar; Investigation, Hussein Almohamad and Ahmed Abdullah Al Dughairi; Resources, Motrih Al-Mutiry, and Hazem Ghassan Abdo; Data curation, subbarayan saravanan, devanantham abijith, parthasarathy kulithalai shiyam sundar and Nagireddy Masthan Reddy; Writing—Original Draft Preparation, Subbarayan Saravanan, Devanantham Abijith, Parthasarathy Kulithalai Shiyam Sundar and Nagireddy Masthan Reddy; Writing—Review And Editing, Hussein Almohamad, Ahmed Abdullah Al Dughairi, Motrih Al-Mutiry And Hazem Ghassan Abdo; Visualization, Hussein Almohamad; supervision, Ahmed Abdullah Al Dughairi, Motrih Al-Mutiry; Project Administration, Hussein Almohamad, Ahmed Abdullah Al Dughairi, Motrih Al-Mutiry and Hazem Ghassan Abdo; Funding Acquisition, Ahmed Abdullah Al Dughairi. All authors have read and agreed to the published version of the manuscript.

Funding: This project was funded by Princess Nourah bint Abdulrahman University Research Supporting Project Number PNURSP2022R24, Princess Nourah bint Abdulrahman University, Riyadh, Saudi Arabia.

Informed Consent Statement: Not applicable.

Data Availability Statement: The data that support the findings of this study are available on request from the corresponding author.

Conflicts of Interest: The authors have no conflicts of interest to declare.

References

- Gori, A.; Lin, N.; Xi, D. Tropical Cyclone Compound Flood Hazard Assessment: From Investigating Drivers to Quantifying Extreme Water Levels. *Earths Future* **2020**, *8*, e2020EF001660. [\[CrossRef\]](#)
- Islam, M.R.; Lee, C.Y.; Mandli, K.T.; Takagi, H. A new tropical cyclone surge index incorporating the effects of coastal geometry, bathymetry and storm information. *Sci. Rep.* **2021**, *11*, 16747. [\[CrossRef\]](#) [\[PubMed\]](#)
- Shultz, J.M.; Shepherd, J.M.; Bagrodia, R.; Espinel, Z.; Shultz, J.M.; Shepherd, J.M. Tropical cyclones in a year of rising global temperatures and a strengthening El Niño. *Disaster Health* **2014**, *2*, 151. [\[CrossRef\]](#) [\[PubMed\]](#)
- Alipour, A.; Yarveysi, F.; Moftakhari, H.; Song, J.Y.; Moradkhani, H. A Multivariate Scaling System Is Essential to Characterize the Tropical Cyclones' Risk. *Earths Future* **2022**, *10*, e2021EF002635. [\[CrossRef\]](#)
- Basheer Ahammed, K.K.; Pandey, A.C. Characterization and impact assessment of super cyclonic storm AMPHAN in the Indian subcontinent through space borne observations. *Ocean. Coast. Manag.* **2021**, *205*, 105532. [\[CrossRef\]](#)
- Hossain, M.S.; Karlson, M.; Neset, T.-S. Application Of Gis For Cyclone Vulnerability Analysis Of Bangladesh. *Earth Sci. Malays. ESMY* **2019**, *3*, 25–34.
- Islam, M.N.; Malak, M.A.; Islam, M.N. Community-based disaster risk and vulnerability models of a coastal municipality in Bangladesh. *Nat. Hazards* **2013**, *69*, 2083–2103. [\[CrossRef\]](#)
- Ghosh, B. Flood susceptibility assessment and mapping in a monsoon-dominated tropical river basin using GIS-based data-driven bivariate and multivariate statistical models and their ensemble techniques. *Environ. Earth Sci.* **2023**, *82*, 28. [\[CrossRef\]](#)
- Knutson, T.; Camargo, S.J.; Chan, J.C.; Emanuel, K.; Ho, C.H.; Kossin, J.; Mohapatra, M.; Satoh, M.; Sugi, M.; Walsh, K.; et al. Tropical Cyclones and Climate Change Assessment: Part II: Projected Response to Anthropogenic Warming. *Bull. Am. Meteorol. Soc.* **2020**, *101*, E303–E322. [\[CrossRef\]](#)
- Reddy, N.M.; Saravanan, S.; Almohamad, H.; Dughairi, A.A.; Al Abdo, H.G. Effects of Climate Change on Streamflow in the Godavari Basin Simulated Using a Conceptual Model including CMIP6 Dataset. *Water* **2023**, *15*, 1701. [\[CrossRef\]](#)
- Reddy, N.M.; Saravanan, S. Extreme precipitation indices over India using CMIP6: A special emphasis on the SSP585 scenario. *Environ. Sci. Pollut. Res.* **2023**, *30*, 47119–47143. [\[CrossRef\]](#) [\[PubMed\]](#)
- Camelo, J.; Mayo, T.L.; Gutmann, E.D. Projected Climate Change Impacts on Hurricane Storm Surge Inundation in the Coastal United States. *Front. Built Environ.* **2020**, *6*, 207. [\[CrossRef\]](#)
- Cha, E.J.; Knutson, T.R.; Lee, T.-C.; Ying, M.; Nakaegawa, T. Third assessment on impacts of climate change on tropical cyclones in the Typhoon Committee Region—Part II: Future projections. *Trop. Cyclone Res. Rev.* **2020**, *9*, 75–86. [\[CrossRef\]](#)
- Knutson, T.; Camargo, S.J.; Chan, J.C.; Emanuel, K.; Ho, C.H.; Kossin, J.; Mohapatra, M.; Satoh, M.; Sugi, M.; Walsh, K.; et al. Tropical cyclones and climate change assessment. *Bull. Am. Meteorol. Soc.* **2019**, *100*, 1987–2007. [\[CrossRef\]](#)

15. Sattar, M.A.; Cheung, K.K.W. Tropical cyclone risk perception and risk reduction analysis for coastal Bangladesh: Household and expert perspectives. *Int. J. Disaster Risk Reduct.* **2019**, *41*, 101283. [[CrossRef](#)]
16. Cardona, O.D.; Van Aalst, M.K.; Birkmann, J.; Fordham, M.; Mc Gregor, G.; Rosa, P.; Pulwarty, R.S.; Schipper, E.L.F.; Sinh, B.T.; Décamps, H.; et al. Determinants of risk: Exposure and vulnerability. In *Managing the Risks of Extreme Events and Disasters to Advance Climate Change Adaptation: Special Report of the Intergovernmental Panel on Climate Change*; Cambridge University Press: Cambridge, UK, 2012; pp. 65–108. ISBN 9781107025066.
17. Peduzzi, P.; Chatenoux, B.; Dao, H.; De Bono, A.; Herold, C.; Kossin, J.; Mouton, F.; Nordbeck, O. Global trends in tropical cyclone risk. *Nat. Clim. Change* **2012**, *2*, 289–294. [[CrossRef](#)]
18. Ahmed, B.; Kelman, I.; Fehr, H.K.; Saha, M. Community Resilience to Cyclone Disasters in Coastal Bangladesh. *Sustainability* **2016**, *8*, 805. [[CrossRef](#)]
19. Hoque MA, A.; Pradhan, B.; Ahmed, N.; Ahmed, B.; Alamri, A.M. Cyclone vulnerability assessment of the western coast of Bangladesh. *Geomat. Nat. Hazards Risk* **2021**, *12*, 198–221. [[CrossRef](#)]
20. Ali, A. Vulnerability of bangladesh to climate change and sea level rise through tropical cyclones and storm surges. *Water Air Soil. Pollut.* **1996**, *92*, 171–179. [[CrossRef](#)]
21. Alam, M.M.; Hossain, M.A.; Shafee, S. Frequency of Bay of Bengal cyclonic storms and depressions crossing different coastal zones. *Int. J. Climatol.* **2003**, *23*, 1119–1125. [[CrossRef](#)]
22. Mohapatra, M. Cyclone hazard proneness of districts of India. *J. Earth Syst. Sci.* **2015**, *124*, 515–526. [[CrossRef](#)]
23. Singh, K.; Panda, J.; Rath, S.S. Variability in landfalling trends of cyclonic disturbances over North Indian Ocean region during current and pre-warming climate. *Appl. Clim.* **2019**, *137*, 417–439. [[CrossRef](#)]
24. Ray, K.; Balachandran, S.; Dash, S.K. Challenges of forecasting rainfall associated with tropical cyclones in India. *Meteorol. Atmos. Phys.* **2022**, *134*, 8. [[CrossRef](#)]
25. Rehman, S.; Sahana, M.; Kumar, P.; Ahmed, R.; Sajjad, H. Assessing hazards induced vulnerability in coastal districts of India using site-specific indicators: An integrated approach. *GeoJournal* **2021**, *86*, 2245–2266. [[CrossRef](#)]
26. Hoque, M.A.; Phinn, S.; Roelfsema, C.; Childs, I. Modelling tropical cyclone hazards under climate change scenario using geospatial techniques. *IOP Conf. Ser. Earth Env. Sci.* **2016**, *47*, 012024. [[CrossRef](#)]
27. Ishtiaque, A.; Eakin, H.; Chhetri, N.; Myint, S.W.; Dewan, A.; Kamruzzaman, M. Examination of coastal vulnerability framings at multiple levels of governance using spatial MCDA approach. *Ocean. Coast. Manag.* **2019**, *171*, 66–79. [[CrossRef](#)]
28. Ali, S.A.; Khatun, R.; Ahmad, A.; Ahmad, S.N. Assessment of Cyclone Vulnerability, Hazard Evaluation and Mitigation Capacity for Analyzing Cyclone Risk using GIS Technique: A Study on Sundarban Biosphere Reserve, India. *Earth Syst. Environ.* **2020**, *4*, 71–92. [[CrossRef](#)]
29. Shankar, S.V.; Dharanirajan, K.; Narshimulu, G. Cyclone vulnerability zonation of southern part of South Andaman, India using Multi-criteria weighted overlay analysis techniques. *IJMS* **2015**, *44*, 1181–1190.
30. Mansour, S.; Darby, S.; Leyland, J.; Atkinson, P.M. Geospatial modelling of tropical cyclone risk along the northeast coast of Oman: Marine hazard mitigation and management policies. *Mar. Policy* **2021**, *129*, 104544. [[CrossRef](#)]
31. Hoque MA, A.; Pradhan, B.; Ahmed, N.; Roy, S. Tropical cyclone risk assessment using geospatial techniques for the eastern coastal region of Bangladesh. *Sci. Total. Environ.* **2019**, *692*, 10–22. [[CrossRef](#)]
32. Mondal, M.; Haldar, S.; Biswas, A.; Mandal, S.; Bhattacharya, S.; Paul, S. Modeling cyclone-induced multi-hazard risk assessment using analytical hierarchical processing and GIS for coastal West Bengal, India. *Reg. Stud. Mar. Sci.* **2021**, *44*, 101779.
33. Mazumdar, J.; Paul, S.K. A spatially explicit method for identification of vulnerable hotspots of Odisha, India from potential cyclones. *Int. J. Disaster Risk Reduct.* **2018**, *27*, 391–405. [[CrossRef](#)]
34. Hossain, M.N. Analysis of human vulnerability to cyclones and storm surges based on influencing physical and socioeconomic factors: Evidences from coastal Bangladesh. *Int. J. Disaster Risk Reduct.* **2015**, *13*, 66–75. [[CrossRef](#)]
35. Jian, W.; Liu, C.; Lam, J.S.L. Cyclone risk model and assessment for East Asian container ports. *Ocean. Coast. Manag.* **2019**, *178*, 104796. [[CrossRef](#)]
36. Abdullah, M.F.; Siraj, S.; Hodgett, R.E. An Overview of Multi-Criteria Decision Analysis (MCDA) Application in Managing Water-Related Disaster Events: Analyzing 20 Years of Literature for Flood and Drought Events. *Water* **2021**, *13*, 1358. [[CrossRef](#)]
37. Malak, M.A.; Sajib, A.M.; Quader, M.A.; Anjum, H. “We are feeling older than our age”: Vulnerability and adaptive strategies of aging people to cyclones in coastal Bangladesh. *Int. J. Disaster Risk Reduct.* **2020**, *48*, 101595. [[CrossRef](#)]
38. Walshe, R.A. ‘Who could have expected such a disaster?’ How responses to the 1892 cyclone determined institutional trajectories of vulnerability in Mauritius. *J. Hist. Geogr.* **2022**, *75*, 55–64. [[CrossRef](#)]
39. Quader, M.A.; Khan, A.U.; Kervyn, M. Assessing Risks from Cyclones for Human Lives and Livelihoods in the Coastal Region of Bangladesh. *Int. J. Environ. Res. Public Health* **2017**, *14*, 831. [[CrossRef](#)]
40. Alam, E.; Collins, A.E. Cyclone disaster vulnerability and response experiences in coastal Bangladesh. *Disasters* **2010**, *34*, 931–954. [[CrossRef](#)]
41. Ghosh, S.; Mistri, B. Cyclone-induced coastal vulnerability, livelihood challenges and mitigation measures of Matla–Bidya inter-estuarine area, Indian Sundarban. *Nat. Hazards* **2023**, *2023*, 3857–3878. [[CrossRef](#)]
42. Mazumdar, J.; Paul, S.K. Socioeconomic and infrastructural vulnerability indices for cyclones in the eastern coastal states of India. *Nat. Hazards* **2016**, *82*, 1621–1643. [[CrossRef](#)]

43. Abraham, A.; Kundapura, S. Evaluating the long-term trends of the climatic variables over three humid tropical basins in Kerala, India. *Arab. J. Geosci.* **2022**, *15*, 811. [[CrossRef](#)]
44. Abijith, D.; Saravanan, S.; Sundar PK, S. Coastal vulnerability assessment for the coast of Tamil Nadu, India—A geospatial approach. *Environ. Sci. Pollut. Res.* **2023**, *30*, 75610–75628. [[CrossRef](#)] [[PubMed](#)]
45. Srinivasa Kumar, T.; Mahendra, R.S.; Nayak, S.; Radhakrishnan, K.; Sahu, K.C. Identification of hot spots and well managed areas of Pichavaram mangrove using Landsat TM and Resourcesat-1 LISS IV: An example of coastal resource conservation along Tamil Nadu Coast, India. *J. Coast. Conserv.* **2012**, *16*, 1–12. [[CrossRef](#)]
46. Parthasarathy, K.S.S.; Deka, P.C. Remote sensing and GIS application in assessment of coastal vulnerability and shoreline changes: A review. *ISH J. Hydraul. Eng.* **2021**, *27*, 588–600. [[CrossRef](#)]
47. Saravanan, S.; Parthasarathy, K.S.S.; Sivaranjani, S. Assessing Coastal Aquifer to Seawater Intrusion: Application of the GALDIT Method to the Cuddalore Aquifer, India. In *Coastal Zone Management: Global Perspectives, Regional Processes, Local. Issues*; Elsevier: Amsterdam, The Netherlands, 2019; pp. 233–250.
48. Saranya, T.; Saravanan, S. Evolution of a hybrid approach for groundwater vulnerability assessment using hierarchical fuzzy-DRASTIC models in the Cuddalore Region, India. *Environ. Earth Sci.* **2021**, *80*, 179. [[CrossRef](#)]
49. Rao, S.R.; Krishna, K.M.; Kumar, O.S.R.U. Study of tropical cyclone “fanoos” using MM5 model-A case study. *Nat. Hazards Earth Syst. Sci.* **2009**, *9*, 43–51.
50. Leijnse, T.W.B.; Giardino, A.; Nederhoff, K.; Caires, S. Generating reliable estimates of tropical-cyclone-induced coastal hazards along the Bay of Bengal for current and future climates using synthetic tracks. *Nat. Hazards Earth Syst. Sci.* **2022**, *22*, 1863–1891. [[CrossRef](#)]
51. Kulithalai Shiyam Sundar, P.; Kundapura, S. Spatial Mapping of Flood Susceptibility Using Decision Tree–Based Machine Learning Models for the Vembanad Lake System in Kerala, India. *J. Water Resour. Plan. Manag.* **2023**, *149*, 04023052. [[CrossRef](#)]
52. Poompavai, V.; Ramalingam, M. Geospatial Analysis for Coastal Risk Assessment to Cyclones. *J. Indian. Soc. Remote. Sens.* **2013**, *41*, 157–176. [[CrossRef](#)]
53. Wilson, K.M.; Baldwin, J.W.; Young, R.M.; Wilson, K.M.; Baldwin, J.W.; Young, R.M. Estimating Tropical Cyclone Vulnerability: A Review of Different Open-Source Approaches. In *Hurricane Risk in a Changing Climate*; Springer: Berlin, Germany, 2022; pp. 255–281.
54. Chou, J.; Dong, W.; Tu, G.; Xu, Y. Spatiotemporal distribution of landing tropical cyclones and disaster impact analysis in coastal China during 1990–2016. *Phys. Chem. Earth Parts A/B/C* **2020**, *115*, 102830. [[CrossRef](#)]
55. Basheer Ahammed, K.K.; Pandey, A.C. Coastal Social Vulnerability and Risk Analysis for Cyclone Hazard Along the Andhra Pradesh, East Coast of India. *KN J. Cart. Geogr. Inf.* **2019**, *69*, 285–303. [[CrossRef](#)]
56. Sobel, A.H.; Wing, A.A.; Camargo, S.J.; Patricola, C.M.; Vecchi, G.A.; Lee, C.Y.; Tippett, M.K. Tropical Cyclone Frequency. *Earths Future* **2021**, *9*, e2021EF002275. [[CrossRef](#)]
57. Mahapatra, M.; Ramakrishnan, R.; Rajawat, A.S. Coastal vulnerability assessment using analytical hierarchical process for South Gujarat coast, India. *Nat. Hazards* **2015**, *76*, 139–159. [[CrossRef](#)]
58. Do, C.; Kuleshov, Y. Multi-Hazard Tropical Cyclone Risk Assessment for Australia. *Remote. Sens.* **2023**, *15*, 795. [[CrossRef](#)]
59. Zhu, J.; Liu, K.; Wang, M.; Xu, W.; Liu, M.; Zheng, J. An empirical approach for developing functions for the vulnerability of roads to tropical cyclones. *Transp. Res. D Transp. Environ.* **2022**, *102*, 103136. [[CrossRef](#)]
60. Kantamaneni, K.; Rani, N.N.V.S.; Rice, L.; Sur, K.; Thayaparan, M.; Kulatunga, U.; Rege, R.; Yenneti, K.; Campos, L.C. A Systematic Review of Coastal Vulnerability Assessment Studies along Andhra Pradesh, India: A Critical Evaluation of Data Gathering, Risk Levels and Mitigation Strategies. *Water* **2019**, *11*, 393. [[CrossRef](#)]
61. Alam, A.; Sammonds, P.; Ahmed, B. Cyclone risk assessment of the Cox’s Bazar district and Rohingya refugee camps in southeast Bangladesh. *Sci. Total Environ.* **2020**, *704*, 135360. [[CrossRef](#)]
62. Hoque MA, A.; Phinn, S.; Roelfsema, C.; Childs, I. Modelling tropical cyclone risks for present and future climate change scenarios using geospatial techniques. *Int. J. Digit. Earth* **2017**, *11*, 246–263. [[CrossRef](#)]
63. Abijith, D.; Saravanan, S. Assessment of land use and land cover change detection and prediction using remote sensing and CA Markov in the northern coastal districts of Tamil Nadu, India. *Environ. Sci. Pollut. Res.* **2022**, *29*, 86055–86067. [[CrossRef](#)]
64. Kulithalai Shiyam Sundar, P.; Deka, P.C. Spatio-temporal classification and prediction of land use and land cover change for the Vembanad Lake system, Kerala: A machine learning approach. *Environ. Sci. Pollut. Res.* **2021**, *29*, 86220–86236. [[CrossRef](#)] [[PubMed](#)]
65. Wolshon, B.; Urbina, E.; Wilmot CLevitan, M. Review of Policies and Practices for Hurricane Evacuation. I: Transportation Planning, Preparedness, and Response. *Nat. Hazards Rev.* **2005**, *6*, 129–142.
66. Tenerelli, P.; Gallego, J.F.; Ehrlich, D. Population density modelling in support of disaster risk assessment. *Int. J. Disaster Risk Reduct.* **2015**, *13*, 334–341. [[CrossRef](#)]
67. Coppola, D.P. *Introduction to International Disaster Management*; Elsevier: Burlington, VT, USA, 2020.
68. Rahman, M.M.; Hossain, M.A.; Ali, M.R.; Ahmed, Z.; Hedayatul Islam, A.H.M. Assessing vulnerability and adaptation strategy of the cyclone affected coastal area of Bangladesh. *Geoenviron. Disasters* **2022**, *9*, 6. [[CrossRef](#)]
69. Rajakumari, S.; Minnu, A.; Sarunjith, K.J. Determination of vulnerable zones along Brahmapur coast, Odisha using AHP and GIS with validation against multiple cyclones. *Environ. Monit. Assess.* **2022**, *194*, 278. [[CrossRef](#)] [[PubMed](#)]

70. Nandi, G.; Neogy, S.; Roy, A.K.; Datta, D. Immediate disturbances induced by tropical cyclone Fani on the coastal forest landscape of eastern India: A geospatial analysis. *Remote. Sens. Appl.* **2020**, *20*, 100407. [[CrossRef](#)]
71. Hoque MA, A.; Phinn, S.; Roelfsema, C.; Childs, I. Tropical cyclone disaster management using remote sensing and spatial analysis: A review. *Int. J. Disaster Risk Reduct.* **2017**, *22*, 345–354. [[CrossRef](#)]
72. Saaty, T.L. That is not the analytic hierarchy process: What the AHP is and what it is not. *J. Multi-Criteria Decis. Anal.* **1997**, *6*, 324–335. [[CrossRef](#)]
73. Saaty, T.L. What is the analytic hierarchy process? In *Mathematical Models for Decision Support*; Springer: Berlin/Heidelberg, Germany, 1988; pp. 109–121.
74. Saaty, T.L. Decision making with the analytic hierarchy process. *Int. J. Serv. Sci.* **2008**, *1*, 83–98. [[CrossRef](#)]
75. Saravanan, S.; Abijith, D.; Reddy, N.M.; Parthasarathy KS, S.; Janardhanam, N.; Sathiyamurthi, S.; Sivakumar, V. Flood susceptibility mapping using machine learning boosting algorithms techniques in Idukki district of Kerala India. *Urban. Clim.* **2023**, *49*, 101503. [[CrossRef](#)]
76. Saravanan, S.; Abijith, D. Flood susceptibility mapping of Northeast coastal districts of Tamil Nadu India using Multi-source Geospatial data and Machine Learning techniques. *Geocarto Int.* **2022**, *37*, 15252–15281. [[CrossRef](#)]
77. UN. *Mitigating Natural Disasters: Phenomena, Effects and Options: A Manual for Policy Makers and Planners*; United Nations: New York, NY, USA, 1991.
78. Sudha Rani, N.N.V.; Satyanarayana, A.N.V.; Bhaskaran, P.K. Coastal vulnerability assessment studies over India: A review. *Nat. Hazards* **2015**, *77*, 405–428. [[CrossRef](#)]
79. Li, K.; Li, G.S. Risk assessment on storm surges in the coastal area of Guangdong Province. *Nat. Hazards* **2013**, *68*, 1129–1139. [[CrossRef](#)]
80. Abijith, D.; Saravanan, S.; Jennifer, J.J.; Parthasarathy, K.S.S.; Singh, L.; Sankriti, R. Assessing the impact of damage and government response toward the cyclone Gaja in Tamil Nadu, India. In *Disaster Resilience and Sustainability*; Elsevier: Amsterdam, The Netherlands, 2021; pp. 577–590.
81. Walsh, K.J.E.; McBride, J.L.; Klotzbach, P.J.; Balachandran, S.; Camargo, S.J.; Holland, G.; Knutson, T.R.; Kossin, J.P.; Lee T cheung Sobel, A.; Sugi, M. Tropical cyclones and climate change. *Wiley Interdiscip. Rev. Clim. Change* **2016**, *7*, 65–89. [[CrossRef](#)]
82. Fakhruddin, B.; Kintada, K.; Hassan, Q. Understanding hazards: Probabilistic cyclone modelling for disaster risk to the Eastern Coast in Bangladesh. *Prog. Disaster Sci.* **2022**, *13*, 100216. [[CrossRef](#)]
83. Parthasarathy, K.S.S.; Deka, P.C.; Saravanan, S.; Abijith, D.; Jacinth Jennifer, J. Assessing the impact of 2018 tropical rainfall and the consecutive flood-related damages for the state of Kerala, India. In *Disaster Resilience and Sustainability: Adaptation for Sustainable Development*; Elsevier: Amsterdam, The Netherlands, 2021; pp. 379–395.
84. Shunmugapriya, K.; Panneerselvam, B.; Muniraj, K.; Ravichandran, N.; Prasath, P.; Thomas, M.; Duraisamy, K. Integration of multi criteria decision analysis and GIS for evaluating the site suitability for aquaculture in southern coastal region, India. *Mar. Pollut. Bull.* **2021**, *172*, 112907. [[CrossRef](#)] [[PubMed](#)]
85. Murty, T.S.; Tadepalli, S.; Aswathanarayana, U.; Nirupama, N. *The Indian Ocean Tsunami*; Taylor & Francis: Boca Raton, FL, USA, 2007.
86. Behera, M.R.; Murali, K.; Sannasiraj, S.A.; Sundar, V. Simulation and prediction of runup heights due to Great Indian Ocean Tsunami. In *Advances in Water Resources and Hydraulic Engineering-Proceedings of 16th IAHR-APD Congress and 3rd Symposium of IAHR-ISHS*; Springer: Berlin/Heidelberg, Germany, 2009; pp. 1244–1249.
87. Saravanan, S.; Parthasarathy, K.S.S.; Vishnuprasath, S.R. Monitoring Spatial and Temporal Scales of Shoreline Changes in the Cuddalore Region, India. In *Coastal Zone Management*; Mu Ramkumar, R., James, A., Menier, D., Kumaraswamy, K., Eds.; Elsevier: Amsterdam, The Netherlands, 2019; pp. 99–112.
88. Parthasarathy, K.S.S.; Saravanan, S.; Deka, P.C.; Devanantham, A. Assessment of potentially vulnerable zones using geospatial approach along the coast of Cuddalore district, East coast of India. *ISH J. Hydraul. Eng.* **2020**, *28*, 422–432. [[CrossRef](#)]
89. Saravanan, S.; Jennifer, J.; Singh, L.; Abijith, D. Cyclone vulnerability assessment of cuddalore coast in Tamil Nadu, India using remote sensing, and GIS. *MATEC Web Conf.* **2018**, *229*, 02022. [[CrossRef](#)]
90. Basheer Ahammed, K.K.; Pandey, A.C.; Parida, B.R.; Wasim Dwivedi, C.S. Impact Assessment of Tropical Cyclones Amphan and Nisarga in 2020 in the Northern Indian Ocean. *Sustainability* **2023**, *15*, 3992. [[CrossRef](#)]
91. Priya, P.; Pattnaik, S.; Trivedi, D. Characteristics of the tropical cyclones over the North Indian Ocean Basins from the long-term datasets. *Meteorol. Atmos. Phys.* **2022**, *134*, 65. [[CrossRef](#)]
92. Singh, K.; Panda, J.; Sahoo, M.; Mohapatra, M. Variability in Tropical Cyclone Climatology over North Indian Ocean during the Period 1891 to 2015. *Asia Pac. J. Atmos. Sci.* **2019**, *55*, 269–287. [[CrossRef](#)]
93. Nair, A.G.; Annadurai, R. A study on various tropical cyclone hits in India—through gis approach. *Int. J. Pure Appl. Math.* **2018**, *119*, 589–595.
94. Deshpande, M.; Singh, V.K.; Ganadhi, M.K.; Roxy, M.K.; Emmanuel, R.; Kumar, U. Changing status of tropical cyclones over the north Indian Ocean. *Clim. Dyn.* **2021**, *57*, 3545–3567. [[CrossRef](#)]
95. Rao, A.D.; Jain, I.; Venkatesan, R. Estimation of Extreme Water Levels Due to Cyclonic Storms: A Case Study for Kalpakkam Coast. *J. Ocean. Clim. Sci. Technol. Impacts* **2016**, *1*, 1–14. [[CrossRef](#)]

96. Karuppusamy, B.; Leo George, S.; Anusuya, K.; Venkatesh, R.; Thilagaraj, P.; Gnanappazham, L.; Kumaraswamy, K.; Balasundareshwaran, A.H.; Balabaskaran Nina, P. Revealing the socio-economic vulnerability and multi-hazard risks at micro-administrative units in the coastal plains of Tamil Nadu, India. *Geomat. Nat. Hazards Risk* **2021**, *12*, 605–630. [[CrossRef](#)]
97. Godschalk, D.R. Urban Hazard Mitigation: Creating Resilient Cities. *Nat. Hazards Rev.* **2003**, *4*, 136–143. [[CrossRef](#)]
98. Mathbor, G.M. Enhancement of community preparedness for natural disasters: The role of social work in building social capital for sustainable disaster relief and management. *Int. Soc. Work* **2007**, *50*, 357–369. [[CrossRef](#)]

Disclaimer/Publisher’s Note: The statements, opinions and data contained in all publications are solely those of the individual author(s) and contributor(s) and not of MDPI and/or the editor(s). MDPI and/or the editor(s) disclaim responsibility for any injury to people or property resulting from any ideas, methods, instructions or products referred to in the content.